J. Fluid Mech. (2004), vol. 515, pp. 135–170. © 2004 Cambridge University Press
DOI: 10.1017/S0022112004000229 Printed in the United Kingdom

Nonlinear geostrophic adjustment of long-wave disturbances in the shallow-water model on the equatorial beta-plane

By J. LE SOMMER[1], G. M. REZNIK[2] AND V. ZEITLIN[1]†
[1]LMD, Ecole Normale Supérieure, 24, rue Lhomond, 75231 Paris Cedex 05, France
[2]P.I. Shirshov Oceanography Institute, Moscow, Russia

(Received 20 October 2003 and in revised form 29 April 2004)

We study the nonlinear response of the equatorial shallow-water system at rest to a localized long-wave perturbation with small meridional to zonal aspect ratio. An asymptotic theory of such a response (adjustment) for small Rossby numbers is constructed. Possible scenarios of nonlinear adjustment are classified depending on the relation between the Rossby number and the aspect ratio. The calculations show that slow, geostrophically balanced Rossby and Kelvin waves and the fast inertia–gravity waves are dynamically split off. The fast component of motion exerts no drag on the slow one, which is proved by direct computation. Evolution equations are derived for both components confirming earlier results which were obtained by ad hoc filtering of one of the components of motion. A well-defined initialization procedure is developed for each component.

Due to the breaking of non-dispersive Kelvin waves, the asymptotic theory has obvious limits of validity. In order to go beyond these limits and to study strongly nonlinear effects during the adjustment process we undertook high-resolution shock-capturing numerical simulations based on recent progress in finite-volume numerical methods. The simulations confirm theoretical results but also reveal new effects such as fission of a strongly nonlinear Rossby-wave packet into a sequence of equatorial modons or jet formation in the wake of a breaking Kelvin wave.

1. Introduction

As is well-known, dynamics of the tropical atmosphere and ocean is a special case due to the change of sign of the Coriolis force at the equator. The response of the tropical atmosphere and ocean at rest to a localized perturbation will therefore be different from the higher latitudes.

On the mid-latitude f- (or β-)plane this response consists of an adjustment of the initial perturbation to a geostrophically balanced vortex state via emission of inertia–gravity waves. The balanced state evolves slowly in time according to (a version of) the standard quasi-geostrophic dynamics. The geostrophic adjustment is one of the fundamental processes in geophysical fluid dynamics (see e.g. Gill 1982). A nonlinear asymptotic theory of geostrophic adjustment in the mid-latitude context was developed recently by Reznik, Zeitlin and Ben Jelloul (2001), and Zeitlin, Reznik & Ben Jelloul (2003) where it was shown that the dynamical separation (splitting)

† Author to whom correspondence should be addressed: zeitlin@lmd.ens.fr

of the fast inertia–gravity waves and slow quasi-geostrophic motions persists over several orders in the Rossby number (see other relevant references on splitting in the above-mentioned papers). The dynamical separation in mid-latitude dynamics may be inferred from the form of the dispersion relation for small perturbations around the rest state with its characteristic spectral gap between the inertia–gravity waves of minimal frequency f and quasi-geostrophic motions of minimal frequency zero.

In the present paper we study the process of geostrophic adjustment and splitting of slow and fast motions on the equatorial β-plane in the framework of the rotating (equatorial) shallow-water model (ERSW). Although the simplest, this model provides a conceptual basis for understanding fundamental processes in the equatorial atmosphere and ocean (cf. e.g. Philander 1990; for a derivation of the ERSW from the equatorial primitive equations see Majda 2003). There has been a recent increase in interest in this model in the context of tropical circulation: Sobel, Nilsson & Polvani (2001); Majda & Klein (2003); Bretherton & Sobel (2003). Usually a reduced, balanced form of the ERSW is used in applications corresponding to the long-wave approximation (Philander 1990). The possibility of such reduction is based on the fact that in the dispersion relation for equatorial waves there is a spectral gap between the slow Kelvin and Rossby waves on the one hand, and the fast inertia–gravity waves and the Yanai wave on the other hand (cf. figure 1 below). As in our previous work we make full technical use of the presence of the spectral gap and, in the context of equatorial geostrophic adjustment, construct an asymptotic theory which allows us to prove dynamical splitting of the balanced and imbalanced components of an arbitrary localized initial perturbation, and to establish its limits.

However, the situation on the equator differs significantly from that of the mid-latitude f-plane because the magnitude of the gap depends on the wavelength and tends to zero with increasing wavenumber. Therefore, asymptotic theory may be consistently developed only for long-wave perturbations (cf. Majda 2003). Thus, we develop an asymptotic (in Rossby number Ro) multi-timescale theory of geostrophic adjustment of a localized perturbation with small aspect ratio δ (meridional over zonal extent). We classify the dynamical regimes arising for different relations between Ro and δ. We completely quantify slow and fast motions, obtain their respective equations of motion with proper initial conditions, and demonstrate their dynamical splitting. The equatorial dynamics sets natural limits on the validity of the asymptotic approach because of the Kelvin wave breaking. To go beyond these limits, we perform high-resolution long-time numerical simulations of the adjustment process which allows extension to fully nonlinear regimes and longer times and better understanding of the details of the adjustment scenario.

The paper is organized as follows. In § 2 after a brief reminder about equatorial shallow-water equations we introduce the characteristic scales and identify slow and fast motions with small aspect ratio. We then analyse qualitatively the dynamical regimes corresponding to different relations between Ro and δ. In § 3 we present the method and the main results of an asymptotic theory of the geostrophic adjustment in the $Ro = O(\delta^2)$ regime. In § 4 we present the results of high-resolution numerical simulations of the equatorial adjustment. Section 5 contains a summary and discussion. A reminder on linear equatorial waves, with special attention paid to the initialization of each type of wave for arbitrary initial conditions, is given in Appendix A as well as some useful formulae for parabolic cylinder functions. Conditions for the mean flow to prevent the Kelvin-wave breaking are presented in Appendix B. The details of calculations of § 3 are presented in Appendix C. The initialization procedure for the $Ro = O(\delta^2)$ nonlinear adjustment regime is presented

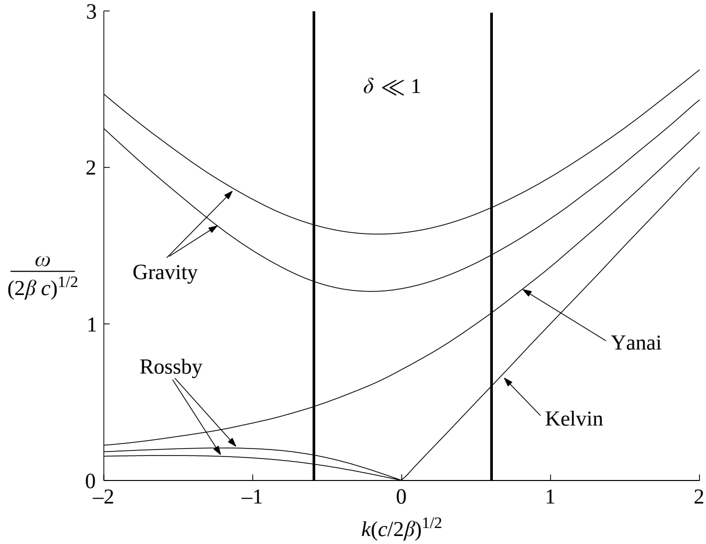

FIGURE 1. Dispersion curves for equatorial waves. c is the phase speed of the Kelvin waves, k is the zonal wavenumber. The domain of long waves is indicated. Two first meridional Rossby modes and two first meridional inertia–gravity waves are shown.

in Appendix D. Appendix E contains the proof of absence of the fast-motion drag onto the slow motions for the $Ro = O(\delta^2)$ adjustment. A brief description of our numerical procedure and a discussion of the Rankine–Hugoniot conditions and potential vorticity changes due to shocks is presented in Appendix F.

2. The long-wave scaling in the ERSW: general considerations and classification of possible dynamical regimes

The ERSW equations are

$$\partial_t \boldsymbol{v} + \boldsymbol{v} \cdot \nabla \boldsymbol{v} + \beta y \hat{\boldsymbol{z}} \wedge \boldsymbol{v} + g \nabla h = 0, \tag{2.1}$$

$$\partial_t h + \nabla \cdot (\boldsymbol{v} h) = 0, \tag{2.2}$$

where $\boldsymbol{v} = (u, v)$ is velocity field, h is the free-surface elevation (for the fluid at rest $h = H_0$), g is acceleration due to gravity and βy is the equatorial Coriolis parameter. Throughout this paper we are interested in the geostrophic adjustment, i.e. the Cauchy problem with given initial conditions:

$$u = u_I(x, y), \;\; v = v_I(x, y), \;\; h = h_I(x, y). \tag{2.3}$$

Everywhere below we impose vanishing boundary conditions at infinity in the meridional direction and systematically use expansions in parabolic cylinder functions $\phi_n(y)$, cf. Appendix A.

The dispersion relation for linear equatorial waves, obtained by linearization of (2.1), (2.2) in Appendix A, displays a spectral gap for the long (in the zonal direction) waves between the Kelvin waves and Rossby waves on the one hand and Yanai and inertia–gravity waves, on the other, cf. figure 1. Therefore, one may assume that for the long-wave part of the spectrum the slow modes (Kelvin, Rossby) are dynamically split from the fast modes (Yanai, inertia–gravity) in the weakly nonlinear regime, as was the case on the mid-latitude f-plane. We will prove this hypothesis below.

2.1. *The choice of scaling*

The long-wave perturbations have a characteristic scale in the zonal direction which is much larger than the meridional one, and we introduce the aspect ratio δ, where

$$\delta = \frac{L_y}{L_x} \ll 1, \quad L_y = \frac{(gH_0)^{1/4}}{\sqrt{\beta}}. \tag{2.4}$$

Correspondingly, the characteristic time and velocity scales are

$$T = \frac{1}{\beta L_y}, \quad U = \frac{g\Delta H}{\beta L_y^2}, \tag{2.5}$$

where ΔH is a typical free-surface displacement, and U is the scale of a typical geostrophically balanced velocity perturbation related to ΔH. The Rossby number $Ro = \epsilon$ is defined as

$$\epsilon = \frac{U}{\beta L_y^2} = \frac{\Delta H}{H_0}. \tag{2.6}$$

The interpretation of this parameter is twofold, as it also has the meaning of the Froude number (cf. Majda & Klein 2003; Majda 2003) if we recall that $\sqrt{gH_0}$ is the typical velocity of the (surface) gravity waves: $\epsilon = U/\sqrt{gH_0}$. Note, that with the scaling (2.4), (2.5) the acceleration, the Coriolis, and the pressure-gradient terms in (2.1) are of the same order. Note also that smallness of the geopotential perturbations (i.e. that of ϵ as defined in (2.6)) is a key ingredient of the weak temperature gradients approximation in studies of the tropical circulation (cf. e.g. Majda & Klein 2003; Bretherton & Sobel 2003) although we never consider below a forced-dissipative problems typical for such studies.

With our scaling the basic equations (2.1), (2.2) take the form

$$u_t + \delta\epsilon u u_x + \epsilon v u_y - yv = -\delta h_x, \tag{2.7}$$

$$v_t + \delta\epsilon u v_x + \epsilon v v_y + yu = -h_y, \tag{2.8}$$

$$h_t + v_y + \delta u_x + \epsilon (hv)_y + \delta\epsilon (hu)_x = 0. \tag{2.9}$$

2.2. *The slow motion: long Rossby and Kelvin waves*

To analyse the long Rossby and Kelvin waves we impose an additional restriction of smallness of the meridional velocity $v \to \delta v$ which follows from linear analysis, cf. Appendix A. For consistency this implies a change of timescale: $t \to t_1 = \delta t$. Therefore, the long Rossby and Kelvin waves are slow and we have

$$u_{t_1} + \epsilon u u_x + \epsilon v u_y - yv = -h_x, \tag{2.10}$$

$$\delta^2 v_{t_1} + \delta^2 \epsilon u v_x + \delta^2 \epsilon v v_y + yu = -h_y, \tag{2.11}$$

$$h_{t_1} + v_y + u_x + \epsilon (hv)_y + \epsilon (hu)_x = 0. \tag{2.12}$$

At the lowest order of the perturbation theory (both ϵ and δ are supposed to be small, their relative value to be fixed below) it follows that

$$u_{t_1}^{(0)} - yv^{(0)} + h_x^{(0)} = 0, \tag{2.13}$$

$$yu^{(0)} + h_y^{(0)} = 0, \tag{2.14}$$

$$h_{t_1}^{(0)} + u_x^{(0)} + v_y^{(0)} = 0, \tag{2.15}$$

thus giving the equations for slow-propagating linear Rossby and Kelvin waves (cf. Appendix A). The next terms of the perturbation series are of the order of

$\max(\delta^2, \epsilon)$. Equations for these terms, with introduction of the corresponding slow time $t_2 = \max(\delta^2, \epsilon) t_1$, are written as follows:

$$u_{t_1}^{(1)} - yv^{(1)} + h_x^{(1)} = -\frac{\epsilon}{\max(\delta^2, \epsilon)} \left(u_{t_2}^{(0)} + u^{(0)} u_x^{(0)} + v^{(0)} u_y^{(0)} \right), \tag{2.16}$$

$$yu^{(1)} + h_y^{(1)} = -\frac{\delta^2}{\max(\delta^2, \epsilon)} v_{t_1}^{(0)}, \tag{2.17}$$

$$h_{t_1}^{(1)} + u_x^{(1)} + v_y^{(1)} = -\frac{\epsilon}{\max(\delta^2, \epsilon)} \left[h_{t_2}^{(0)} + \left(h^{(0)} u^{(0)} \right)_x + \left(h^{(0)} v^{(0)} \right)_y \right]. \tag{2.18}$$

Let us analyse qualitatively what the different asymptotic relations between the parameters ϵ and δ imply for Rossby waves.

If $\delta^2 \gg \epsilon$, equations (2.16)–(2.18) become linear. Because it is the term $v_{t_1}^{(0)}$ on the right-hand side of (2.17) which provides dispersion in the system, within this range of parameters dispersion overcomes nonlinearity and, in the context of the geostrophic adjustment, any initial packet of Rossby waves will be dispersed.

If $\delta^2 \ll \epsilon$ the nonlinearity overcomes dispersion. General properties of this regime were recently presented by Majda (2003).

A non-compensated nonlinearity usually means breaking. However, the precise dynamical meaning of this process is not clear at this stage. For instance, it is known that equatorial modons may exist for strong nonlinearities (Boyd 1985). Does equatorial adjustment with subsequent Rossby-wave ‘breaking’ produce them in this regime? We give some elements of the answer below.

Finally, at $\delta^2 \sim \epsilon$, the advective nonlinearity and dispersion may compensate each other and form solitary waves from the initial perturbation in the Rossby-wave part of the spectrum. A typical equation combining the effects of weak nonlinearity and weak dispersion is the Korteweg-de Vries (KdV) or modified Korteweg-de Vries (mKdV) and one may expect that the Rossby-wave packet will obey one of them in this regime and form solitons (Boyd 1980*a*)

The long Kelvin waves should always break (Boyd 1980*b*; Ripa 1982), because they are defined by the condition $v^{(0)} = 0$ and are, thus, non-dispersive whatever the relation between δ and ϵ. Their breaking, therefore, consists of the formation of a hydraulic jump. The breaking of Kelvin waves may be prevented by a fine-tuned mean zonal flow (Boyd 1984). This situation is discussed in Appendix B.

2.3. *The fast motion: long inertia–gravity and Yanai waves*

For these waves $u \sim v$ and equations (2.7)–(2.9) remain unchanged. At the lowest order we have

$$u_t^{(0)} - yv^{(0)} = 0, \tag{2.19}$$

$$v_t^{(0)} + yu^{(0)} + h_y^{(0)} = 0, \tag{2.20}$$

$$h_t^{(0)} + v_y^{(0)} = 0. \tag{2.21}$$

A single equation for $v^{(0)}$ follows from this system (cf. Gill 1980):

$$v_{tt}^{(0)} + y^2 v^{(0)} - v_{yy}^{(0)} = 0, \tag{2.22}$$

which has the following solution in terms of the parabolic cylinder functions $\phi_n(y)$:

$$v^{(0)} = \sum_{n=0}^{\infty} v_n^{(0)}(x, t) \phi_n(y), \quad v_n^{(0)} = A_{0_n}^{+}(x, t_1) \mathrm{e}^{\mathrm{i}\sigma_n t} + \text{c.c}, \quad \sigma_n = \sqrt{2n+1}. \tag{2.23}$$

Thus, at the lowest order we obtain non-propagating oscillations with frequencies σ_n which are well separated from the zero frequency (in the fast time t) of long Rossby and Kelvin waves (cf. figure 1).

In the limit $\epsilon \to 0$, i.e. neglecting nonlinearity in (2.7)–(2.9), the next approximation in δ gives a non-dispersive eastward propagation of the envelope A_{0_n} in the slow time $t_1 = \delta t$:

$$A^{\pm}_{0_n} = A^{\pm}_{0_n}\left(x - \frac{t_1}{2\sigma_n^2}\right) \tag{2.24}$$

which is consistent with the group velocity estimate for long waves (cf. figure 1. At the next order in δ dispersion will give rise to evolution in $t_2 = \delta^2 t$.

If, on the other hand, the limit $\delta \to 0$ is taken in (2.7)–(2.9) (infinitely long waves), the resonances generated by nonlinearity appear only at $O(\epsilon^2)$ because, as easily seen from (2.23), the $O(\epsilon)$ bilinear combinations of the oscillations of the form (2.23) are non-resonant:

$$\sqrt{2k+1} \neq \sqrt{2l+1} \pm \sqrt{2m+1} \tag{2.25}$$

for any integer k, l, m. At the same time, the cubic combinations appearing at $O(\epsilon^2)$ do produce resonances.

Hence, in order to counter-balance the dispersion of the envelope of the fast waves by nonlinearity we need to have $\delta \sim \epsilon$. In this regime one can expect that the dynamics of the envelope A_{0_n} in t_2, as is usual for a weakly nonlinear envelope evolution, obeys the nonlinear Schrödinger equation, or a system of coupled Schrödinger equations if the simultaneous evolution of several modes of the type (2.23) is considered. Thus formation of the envelope solitons (cf. Boyd 1983) is possible. Under the condition of very weak dispersion, $\delta \ll \epsilon$, the nonlinear interactions give a small frequency shift (no breaking). Under the condition of strong dispersion, $\delta \gg \epsilon$, the envelope A_{0_n} is slowly dispersed.

2.4. *A summary of possible weakly nonlinear dynamical regimes in the long-wave approximation*

In the absence of mean flow the results of the preceding qualitative analysis may be summarized as follows

For Rossby numbers up to δ^2 Rossby waves are dispersed as well as the envelope of the gravity waves; Kelvin waves break forming hydraulic jumps.

For Rossby numbers of order δ^2 Rossby waves form solitons, the envelope of the gravity waves is dispersed and Kelvin waves break.

For Rossby numbers in the interval (δ^2, δ) Rossby and Kelvin waves break, the envelope of the gravity waves is dispersed.

For Rossby numbers of the order of δ, Rossby and Kelvin waves break, the envelope of the gravity waves obeys the nonlinear Schrödinger equation and forms modulation solitons.

For Rossby numbers greater than δ Rossby and Kelvin waves break and the envelope of the gravity waves has a nonlinear frequency shift.

We have performed an asymptotic analysis of all the aforementioned regimes which confirms these qualitative conclusions. As the dynamically most interesting example (appearance of Rossby solitons) we present below a detailed analysis of the regime $\epsilon \sim \delta^2$. For typical Rossby numbers of order 0.1 for the balanced motions in the equatorial atmosphere (cf. e.g. Majda & Klein 2003) and of order 0.3 for the ocean (cf. e.g. Boyd 1980) the typical horizontal scales in this regime correspond to thousands of kilometres (planetary-scale perturbations) in the atmosphere and to hundreds of kilometres (mesoscale) in the ocean. They are, hence, appropriate e.g. for the oceanic perturbations due to equatorial westerly wind bursts (cf. Philander 1990).

3. The long-wave adjustment at $Ro = O(\delta^2)$

In this regime, the basic equations (2.7)–(2.9) take the form

$$u_t + \delta^3 u u_x + \delta^2 v u_y - y v = -\delta h_x, \tag{3.1}$$

$$v_t + \delta^3 u v_x + \delta^2 v v_y + y u = -h_y, \tag{3.2}$$

$$h_t + v_y + \delta u_x + \delta^2 (hv)_y + \delta^3 (hu)_x = 0. \tag{3.3}$$

We analyse below the geostrophic adjustment in this system at the first four orders in δ. A solution of (3.1)–(3.3) is sought in the form of an asymptotic series in δ:

$$u = u^{(0)}(x, y, t, t_1, t_2, \ldots) + \delta u^{(1)}(x, y, t, t_1, t_2, \ldots) + \ldots, \tag{3.4}$$

and similarly for the fields v and h. Here the slow timescales $t_1 = \delta t,\ t_2 = \delta^2 t, \ldots$ are introduced. Each field $f(x, y, t, t_1, t_2, \ldots)$ is represented as a sum of the slow component $\bar{f}(x, y, t_1, t_2, \ldots)$ defined as the average of f over the fast time t, and the fast component $\tilde{f} = f - \bar{f}$. At each order we describe the evolution of both slow and fast components of the flow and show how to split the initial conditions unambiguously and obtain well-posed Cauchy problems for both components. The fast and slow variables are not mutually independent due to nonlinearity: the slow evolution of the fast fields depends on the slow ones (guiding) and, in principle, the self-interaction of the fast components should influence the slow fields. However, we show (and this is the most imortant theoretical result of the paper) that at least at the leading order there is no fast-component drag upon the slow component.

In the next subsection we explain the general scheme of calculations. Technical details are relegated to Appendix C. The initialization procedure is presented in the Appendix D. Note that results obtained at order n provide a description of the system for times up to $1/(\delta^{n+1}T)$. Readers not interested in technical details can proceed directly to § 3.2.

It should be noted that the results on the slow motion itself which we obtain below are well-known: the KdV dynamics of weakly nonlinear equatorial Rossby waves (3.37) was discovered by Boyd (1980*a*). The overturning of the equatorial Kelvin waves (3.38) was also demonstrated about 20 years ago by Boyd (1980*b*) and Ripa (1982). However, these studies started from a situation close to the geostrophic balance, i.e. they filtered the fast component of motion from the beginning. The novelty of our approach is that without any filtering we prove that fast and slow motions are dynamically split and the old results are consistent. We also complete them by providing the corresponding evolution of the fast component.

3.1. *The method*

Equations for the nth approximation are taken in the form

$$u_t^{(n)} - y v^{(n)} + u_{t_1}^{(n-1)} + h_x^{(n-1)} = P_u^{(n)}, \tag{3.5}$$

$$v_t^{(n)} + y u^{(n)} + h_y^{(n)} = P_v^{(n)}, \tag{3.6}$$

$$h_t^{(n)} + h_{t_1}^{(n-1)} + v_y^{(n)} + u_x^{(n-1)} = P_h^{(n)}. \tag{3.7}$$

Simultaneously the equation for v from the previous step is used:

$$v_t^{(n-1)} + y u^{(n-1)} + h_y^{(n-1)} = P_v^{(n-1)}. \tag{3.8}$$

Here, by definition,

$$u^{(-1)} = v^{(-1)} = h^{(-1)} = 0, \quad P_u^{(-1)} = P_v^{(-1)} = P_h^{(-1)} = 0, \tag{3.9}$$

and the right-hand sides for the first three orders are

$$P_u^{(0)} = P_v^{(0)} = P_h^{(0)} = 0, \tag{3.10}$$

$$P_u^{(1)} = 0, \quad P_v^{(1)} = -v_{t_1}^{(0)}, \quad P_h^{(1)} = 0, \tag{3.11}$$

$$\begin{aligned} P_u^{(2)} = -u_{t_2}^{(0)} - v^{(0)}u_y^{(0)}, \quad P_v^{(2)} &= -\left(v_{t_2}^{(0)} + v_{t_1}^{(1)} + v^{(0)}v_y^{(0)}\right), \\ P_h^{(2)} &= -h_{t_2}^{(0)} - \left(h^{(0)}v^{(0)}\right)_y, \end{aligned} \tag{3.12}$$

$$P_u^{(3)} = -u_{t_3}^{(0)} - u_{t_2}^{(1)} - v^{(1)}u_y^{(0)} - v^{(0)}u_y^{(1)} - u^{(0)}u_x^{(0)}, \tag{3.13}$$

$$P_h^{(3)} = -h_{t_3}^{(0)} - h_{t_2}^{(1)} - \left(h^{(0)}v^{(1)} + h^{(1)}v^{(0)}\right)_y - \left(h^{(0)}u^{(0)}\right)_x, \tag{3.14}$$

and we will not need the explicit expression for $P_v^{(3)}$ in what follows. We obtain, by averaging (3.5)–(3.8), the following equations for the slow fields:

$$\bar{u}_{t_1}^{(n-1)} + \bar{h}_x^{(n-1)} - y\bar{v}^{(n)} = \bar{P}_u^{(n)}, \tag{3.15}$$

$$y\bar{u}^{(n)} + \bar{h}_y^{(n)} = \bar{P}_v^{(n)}, \tag{3.16}$$

$$\bar{h}_{t_1}^{(n-1)} + \bar{u}_x^{(n-1)} + \bar{v}_y^{(n)} = \bar{P}_h^{(n)}, \tag{3.17}$$

$$y\bar{u}^{(n-1)} + \bar{h}_y^{(n-1)} = \bar{P}_v^{(n-1)}. \tag{3.18}$$

Among these equations (3.15), (3.17), and (3.18) are sufficient to determine the slow motion, while (3.16) will be used to define the fast motion in the next approximation. Correspondingly, for the fast fields we obtain

$$\tilde{u}_t^{(n)} - y\tilde{v}^{(n)} = \tilde{P}_u^{(n)} - \tilde{u}_{t_1}^{(n-1)} - \tilde{h}_x^{(n-1)} \equiv \tilde{R}_u^{(n)}, \tag{3.19}$$

$$\tilde{v}_t^{(n)} + y\tilde{u}^{(n)} + \tilde{h}_y^{(n)} = \tilde{P}_v^{(n)} \equiv \tilde{R}_v^{(n)}, \tag{3.20}$$

$$\tilde{h}_t^{(n)} + \tilde{v}_y^{(n)} = \tilde{P}_h^{(n)} - \tilde{h}_{t_1}^{(n-1)} - \tilde{u}_x^{(n-1)} \equiv \tilde{R}_h^{(n)}. \tag{3.21}$$

The key idea is to solve for the variable $\bar{v}^{(n)}$ first, and then to determine $\bar{u}^{(n-1)}$ and $\bar{h}^{(n-1)}$. By differentiating and combining equations (3.15)–(3.18) we can obtain a single equation for $\bar{v}^{(n)}$:

$$\left(\bar{v}_{yy}^{(n)} - y^2\bar{v}^{(n)}\right)_{t_1} + \bar{v}_x^{(n)} = \left(y\bar{P}_u^{(n)} + \bar{P}_{h_y}^{(n)} - \bar{P}_{v_{t_1}}^{(n-1)}\right)_{t_1} - \left(y\bar{P}_h^{(n)} + \bar{P}_{u_y}^{(n)} - \bar{P}_{v_x}^{(n-1)}\right)_x, \tag{3.22}$$

and an equation for its initial value $\bar{v}_I^{(n)}$:

$$\bar{v}_{I_{yy}}^{(n)} - y^2\bar{v}_I^{(n)} = \left(\bar{u}_{I_y}^{(n-1)} + y\bar{h}_I^{(n-1)}\right)_x + \left(y\bar{P}_u^{(n)} + \bar{P}_{h_y}^{(n)} - \bar{P}_{v_{t_1}}^{(n-1)}\right)_I. \tag{3.23}$$

As usual, the slow evolution follows from removal of resonant terms on the right-hand side of (3.22). We proceed by subsequent averaging of this equation in t_2, t_3 to determine the corresponding evolution in slow times of the previous-order slow components. After resonances are removed, equation (3.22) can be solved and $\bar{v}^{(n)}$ determined. It should be stressed that the analysis of resonances on the right-hand side of (3.22) allows only the slow evolution of the Rossby-wave part of the perturbation to be fixed, because the linear operator on the left-hand side of this equation corresponds precisely to Rossby waves. To describe the slow evolution of the Kelvin-wave part we add equations (3.15) and (3.17) and obtain

$$\left(\bar{u}^{(n-1)}+\bar{h}^{(n-1)}\right)_{t_1}+\left(\bar{u}^{(n-1)}+\bar{h}^{(n-1)}\right)_x=-\bar{v}^{(n)}_y+y\bar{v}^{(n)}+\bar{P}^{(n)}_u+\bar{P}^{(n)}_h. \tag{3.24}$$

The linear operator on the right-hand side here corresponds to Kelvin waves and the resonances are absent if

$$\left[\bar{v}^{(n)}_y-y\bar{v}^{[n]}\right]_{(K)}=\left[\bar{P}^{(n)}_u+\bar{P}^{(n)}_h\right]_{(K)}, \tag{3.25}$$

where the subscript (K) means that only the terms $\propto U(x-t_1)$ (cf. (3.32) below) are considered in the bracketed expression. A bounded solution of this equation exists if

$$\int_{-\infty}^{+\infty}\mathrm{d}y\,\phi_0\left[\bar{P}^{[n)}_u+\bar{P}^{(n)}_h\right]_{(K)}=0, \tag{3.26}$$

which gives a slow evolution of the Kelvin waves of preceding orders (see below and Appendix C).

Knowing $\bar{v}^{(n)}$ and having removed resonances from the right-hand side of (3.15), (3.17), and (3.18) we may find $\bar{u}^{(n-1)}$ and $\bar{h}^{(n-1)}$ from (3.15), and (3.17), and thus determine the slow component of motion at the given order. The order $(n-1)$ slow component is a sum of free Rossby and Kelvin waves and some 'forced' terms generated by nonlinear interactions of preceding-order fields. The slow evolution of order $(n-1)$ Rossby and Kelvin waves is determined from the analysis of the $(n+1)$th order, etc.

The same strategy is used for the fast component. From (3.19)–(3.21) we obtain an equation for $\tilde{v}^{(n)}$:

$$\tilde{v}^{(n)}_{tt}+y^2\tilde{v}^{(n)}-\tilde{v}^{(n)}_{yy}=\tilde{R}^{(n)}_{v_t}-\tilde{R}^{(n)}_{h_y}-y\tilde{R}^{(n)}_u, \tag{3.27}$$

with initial conditions:

$$\tilde{v}^{(n)}_I=-\bar{v}^{(n)}_I, \tag{3.28}$$

$$\tilde{v}^{(n)}_t\big|_{t=0}=-\left[yu^{(n)}+h^{(n)}_y-P^{(n)}_v\right]_{t=0}. \tag{3.29}$$

Removal of resonances from the right-hand side of this equation gives slow evolution of the fast variables. The linear operator on the l.h.s. corresponds to inertia–gravity and Yanai waves. Hence, the dependence on slow times of these fast waves, i.e. modulation, will be thus determined. After removal of resonances equation (3.27) may be solved and $\tilde{v}^{(n)}$ determined. Knowing $\tilde{v}^{(n)}$, $\tilde{u}^{(n)}$ and $\tilde{h}^{(n)}$ may be found from (3.19) and (3.21).

It is easy to see that the fast and the slow variables are not mutually independent. The right-hand side of (3.27) contains terms of the form $\bar{u}^{(k)}\tilde{v}^{(m)}$, $k,m<n$ and, therefore, the slow evolution of the fast fields depends on slow fields (guiding). In turn, the right-hand side of equations (3.15)–(3.18) contains terms of the type $\langle\tilde{u}^{(k)}\tilde{v}^{(m)}\rangle$ and, in principle, the fast motion should influence the slow motion.

3.2. *The main results*

3.2.1. *Fast motion*

We show (see Appendix C) that the fast motion consists of (infinitely) long inertia–gravity and Yanai waves of the form (2.23). The slow-time dependence of the modulated amplitude A_{0_n} is given by (2.24). At the next approximation A_{0_n} acquires a nonlinear frequency shift and a frequency shift due to the mean zonal flow represented by $\Phi^{(M)}$, cf. Appendix C:

$$A^{\pm}_{0_{n_{t_2}}} \pm \frac{i}{2\sigma_n}\left(1 - \frac{3}{4\sigma_n^4}\right) A^{\pm}_{0_{n_{xx}}} \pm \frac{\mathrm{i}}{2\sigma_n}\Phi^{(M)}_{nn} A^{\pm}_{0_n} = 0. \tag{3.30}$$

The first correction to the amplitude obeys the following equation:

$$A^{\pm}_{1_{n_{t_1}}} + \frac{1}{2\sigma_n^2} A^{\pm}_{1_{n_x}} = \mp\frac{\mathrm{i}}{2\sigma_n}\left(\Phi^{(K)}_{nn}(x, t_1) + \Phi^{(R)}_{nn}(x, t_1)\right) A^{\pm}_{0_n}, \tag{3.31}$$

where $\Phi^{(K)}, \Phi^{(R)}$ represent contributions from the slow Kelvin and Rossby waves, respectively, cf. Appendix C. Thus, the modulation of the fast component is guided by the slow one.

3.2.2. *Slow motion*

The full slow solution $(\bar{u}^{(0)}, \bar{v}^{(1)}, \bar{h}^{(0)})$ is a sum of three contributions. All of them are unambiguously defined. The first one, $(\bar{u}^{(0)}_{(K)}, 0, \bar{h}^{(0)}_{(K)})$ is the eastward-propagating Kelvin-wave part:

$$\bar{u}^{(0)}_{(K)} = \bar{h}^{(0)}_{(K)} = U_0(x - t_1)\phi_0(y). \tag{3.32}$$

The second one is the westward-propagating Rossby-wave part $(\bar{u}^{(0)}_{(R)}, \bar{v}^{(1)}_{(R)}, \bar{h}^{(0)}_{(R)})$:

$$\bar{u}^{(0)}_{(R)} = \frac{1}{2}\sum_{n=1}^{\infty} \bar{\mathscr{V}}_{1_n}(x + \bar{c}_n t_1)\left[\frac{\sqrt{2(n+1)}}{1+\bar{c}_n}\phi_{n+1}(y) - \frac{\sqrt{2n}}{1-\bar{c}_n}\phi_{n-1}(y)\right], \tag{3.33}$$

$$\bar{v}^{(1)}_{(R)} = \sum_{n=1}^{\infty} \bar{v}^{(1)}_n(x + \bar{c}_n t_1)\phi_n(y), \tag{3.34}$$

$$\bar{h}^{(0)}_{(R)} = \frac{1}{2}\sum_{n=1}^{\infty} \bar{\mathscr{V}}_{1_n}(x + \bar{c}_n t_1)\left[\frac{\sqrt{2(n+1)}}{1+\bar{c}_n}\phi_{n+1}(y) + \frac{\sqrt{2n}}{1-\bar{c}_n}\phi_{n-1}(y)\right], \tag{3.35}$$

where $\bar{\mathscr{V}}_{1_{n_x}} = \bar{v}^{(1)}_n$, and $\bar{c}_n = 1/(2n+1) = \sigma_n^2$. The third one is an arbitrary geostrophically balanced zonal flow $(\bar{u}^{(0)}_{(M)}, 0, \bar{h}^{(0)}_{(M)})$:

$$y\bar{u}^{(0)}_{(M)} + \bar{h}^{(0)}_{(M)_y} = 0. \tag{3.36}$$

The slow evolution of the Rossby-wave component is given by the KdV equation

$$\bar{\mathscr{V}}_{1_{n_{t_3}}} + \alpha_n \bar{\mathscr{V}}_{1_{n_{xxx}}} + \beta_n \bar{\mathscr{V}}_{1_n}\bar{\mathscr{V}}_{1_{n_x}} = 0. \tag{3.37}$$

The coefficients α_n, β_n of the KdV equation are constants depending only on the meridional structure of the mode (see Appendix C for details). Hence the Rossby-wave component of the initial localized perturbation will split into a sequence of westward-propagating solitons.

The slow evolution of the Kelvin-wave component is given by the Riemann wave equation

$$U_{0_{t_3}} + \frac{1}{\pi^{1/4}}\sqrt{\frac{3}{2}}\, U_0 U_{0_x} = 0 \tag{3.38}$$

leading to overturning in finite time (in terms of the third slow time t_3).

3.2.3. *Fast–slow motion splitting*

The results obtained for the slow motion are rather surprising, because the evolution equations (3.37) and (3.38) do not contain any trace of the fast component, in spite of the aforementioned influence of the fast fields upon the slow ones. We prove by a direct calculation in Appendix E that the averaged fast–fast terms are not resonant and, hence, make no contribution (drag) to the slow-field evolution equations at least up to times $O(\delta^{-4}T)$. Thus, we demonstrate that the slow and the fast motions are dynamically split and justify the naive filtering (i.e. throwing away) of the fast waves which provides a 'fast-track' derivation of (3.37) and (3.38).

3.3. *Discussion of the asymptotic theory results*

Thus, detailed calculations confirm the scenario proposed in § 2 for the regime $Ro \sim \delta^2$. We have shown that an arbitrary long-wave equatorial perturbation with small characteristic Rossby number splits into fast and slow components. The former is a packet of inertia–gravity and Yanai waves with a Doppler-shift due to the slow components and a nonlinear frequency shift. The fast component does not influence the slow one. The latter is a combination of Rossby and Kelvin waves propagating in opposite directions along the equator and obeying their own modulation equations. For Rossby waves the evolution equation is KdV which is known to produce a sequence of solitons from a localized initial disturbance. For Kelvin waves the evolution equation is a simple-wave equation which produces overturning in finite time. Thus, within the limits of validity of the non-dissipative asymptotic theory, i.e. for times of the order $1/(\delta^3 T)$ the dynamical splitting of slow and fast components is proved. Note that going farther in the asymptotic expansions does not make sense as the asymptotic theory breaks down once Kelvin waves overturn and generate smaller characteristic scales.

Therefore, we have given a proof that the filtering of the fast component applied in the works of Boyd (1980*a*, *b*) and Ripa (1982) is legitimate and that the fast motion exerts no drag (up to times $O(1/\delta^3 T)$) upon the slow motion. However, as was just mentioned, the non-dissipative asymptotic theory has intrinsic limitations due to the breaking of Kelvin waves. For localized initial disturbances on the infinite equatorial beta-plane these limitations do not affect the westward-moving Rossby-wave part of the perturbation much, as Kelvin waves move in the opposite direction. However, for the eastward-moving part of the perturbation the overturning of the Kelvin waves will, presumably, destroy splitting. Even for the Rossby-wave part of the spectrum the question of persistence of non-interaction with the fast waves arises for times much greater than $1/(\delta^3 T)$. The practical question of robustness of the asymptotic theory also arises (as its convergence cannot be proved), i.e. the question of the behaviour of the system for small but finite Ro and δ. It should be emphasized that certain dynamical phenomena cannot be described by the single-spatial-scale theory of preceding sections by construction, for instance the non-local resonant interactions of triads including very short and very long equatorial waves (Ripa 1982). Another question beyond the limits of the present theory is that of Rossby-wave breaking for strong nonlinearities with possible formation of modons, which was already mentioned in § 3.

In order to test the predictions of our theory and to go beyond its formal limits we have undertaken a high-resolution numerical simulation of the geostrophic adjustment in the equatorial shallow-water model.

4. High-resolution numerical simulations of the equatorial adjustment problem

When performing numerical simulations of the equatorial adjustment problem it is important to resolve well both large and small scales simultaneously, and not to

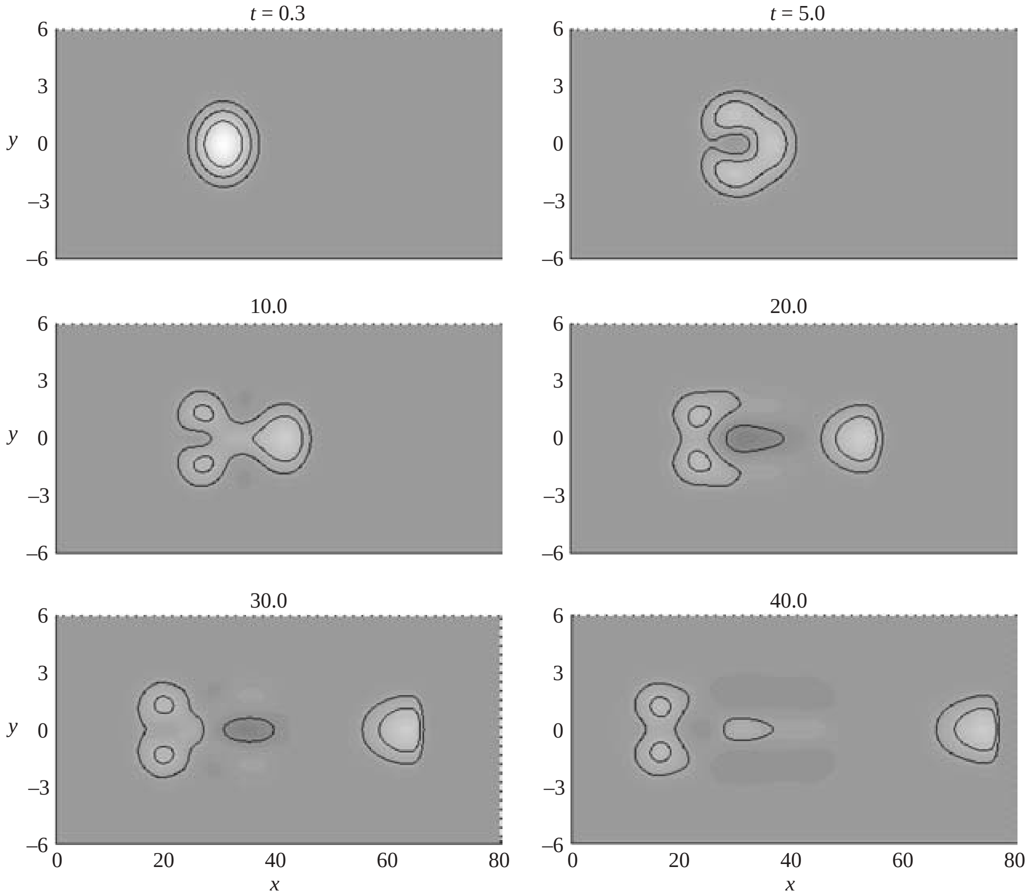

FIGURE 2. Adjustment of a localized large-scale height anomaly symmetric with respect to the equator. The Rossby-wave part of the initial perturbation is moving west, the Kelvin-wave part is moving east and breaks in finite time forming a shock. A packet of inertia–gravity waves centred at the location of the initial perturbation's maximum ($x = 30$) is slowly dispersed. The isolines of h at values 0.98, 1.02, 1.05, 1.1 are shown at each panel. Here and below darker (lighter) shading represents negative (positive) height anomaly, respectively.

lose resolution for long enough times. It is crucial to have a reliable shock-capturing scheme allowing resolution of the wave-breaking process. The recent progress in the development of finite-volume shock-capturing numerical schemes for shallow-water problems (Audusse *et al.* 2003) provides an optimal framework for such studies (see Appendix F).

4.1. *The adjustment process*

The first numerical simulation we performed was to test a general scenario of equatorial adjustment in the case of moderate/strong nonlinearities. We start from a localized large-scale height perturbation with no initial velocity ($h_I = h_I(x, y), u_I = v_I = 0$). The initial height field is Gaussian, with meridional extent L_y, aspect ratio $\delta = 0.3$, and maximal non-dimensional amplitude (Rossby number) $\Delta H/H_0 = 0.3$ with $H_0 = 1$. The initial perturbation is symmetric with respect to the equator. For simplicity of calculation the zonal boundary conditions are periodic. In figure 2 we present the evolution of this perturbation up to $40T$. The length unit in all figures

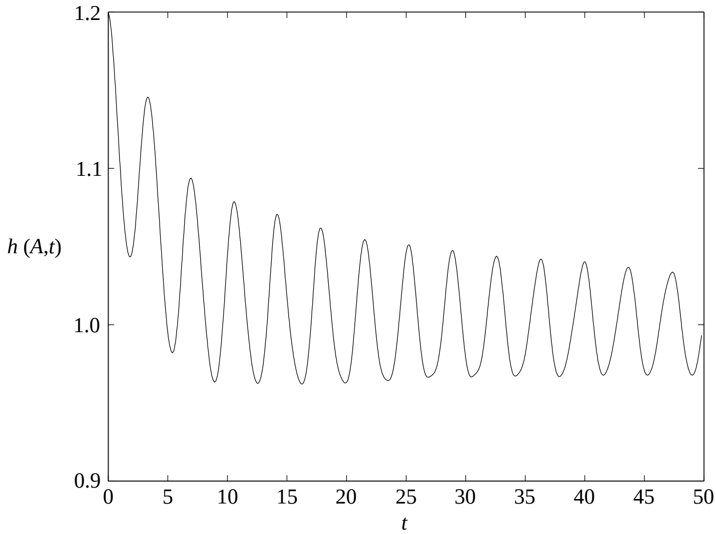

FIGURE 3. Fast oscillations, as measured at the initial perturbation location at $x_0 = 30$, $y_0 = 0$.

below is L_y (cf. (2.4)), the time scale is T (cf. (2.5)). The simulation shows that the initial perturbation rapidly splits to form a westward-moving Rossby-wave packet, an eastward-moving Kelvin wave, and a slowly dispersing packet of inertia–gravity waves. Kelvin- and Rossby-wave parts have Rossby numbers of order 0.1. The Kelvin wave breaks forming a sharp front (Kelvin front) but the breaking does not produce much gravity-wave activity – but see below. The fast oscillations are observed for the whole run duration, cf. figure 3. Their frequency corresponds to that of the lowest inertia–gravity mode on figure 1. This is the fast part of the motion, as the initial conditions have a non-zero projection onto the fast component – cf. Appendix D. Mutual advection apart, no significant interaction between slow and fast motions is observed. We thus see that the slow–fast splitting remains valid for not too small δ and Ro and that although the Kelvin wave breaks this does not significantly change the adjustment scenario.

4.2. *Kelvin-wave breaking*

To study the process of Kelvin-wave breaking in more detail we performed numerical simulations of the evolution of the pure nonlinear Kelvin wave, with $v_I = 0$, the same h_I as in the previous simulation, but with u_I obeying (A 16) exactly. This simulation is presented in figure 4. The simulation shows the formation of a wake of short-scale inertia–gravity waves behind the Kelvin front. This is a new phenomenon arising beyond the limits of the asymptotic theory, as discussed above. The phenomenon was qualitatively explained by Fedorov & Melville (2000), who were first to perform high-resolution numerical simulations of Kelvin fronts. A necessary condition for such an emission is that the phase speed of the nonlinear Kelvin wave (which is greater than the phase speed of linear Kelvin waves due to nonlinearity) is large enough to be equal to the inertia–gravity-wave phase velocity (cf. figure 1). The corresponding wavelength for emitted inertia–gravity waves may be estimated from the intersection of the (nonlinearly boosted) Kelvin-wave curve and upper curves for inertia–gravity waves on figure 1. The parameters of inertia–gravity waves on figure 4 are consistent

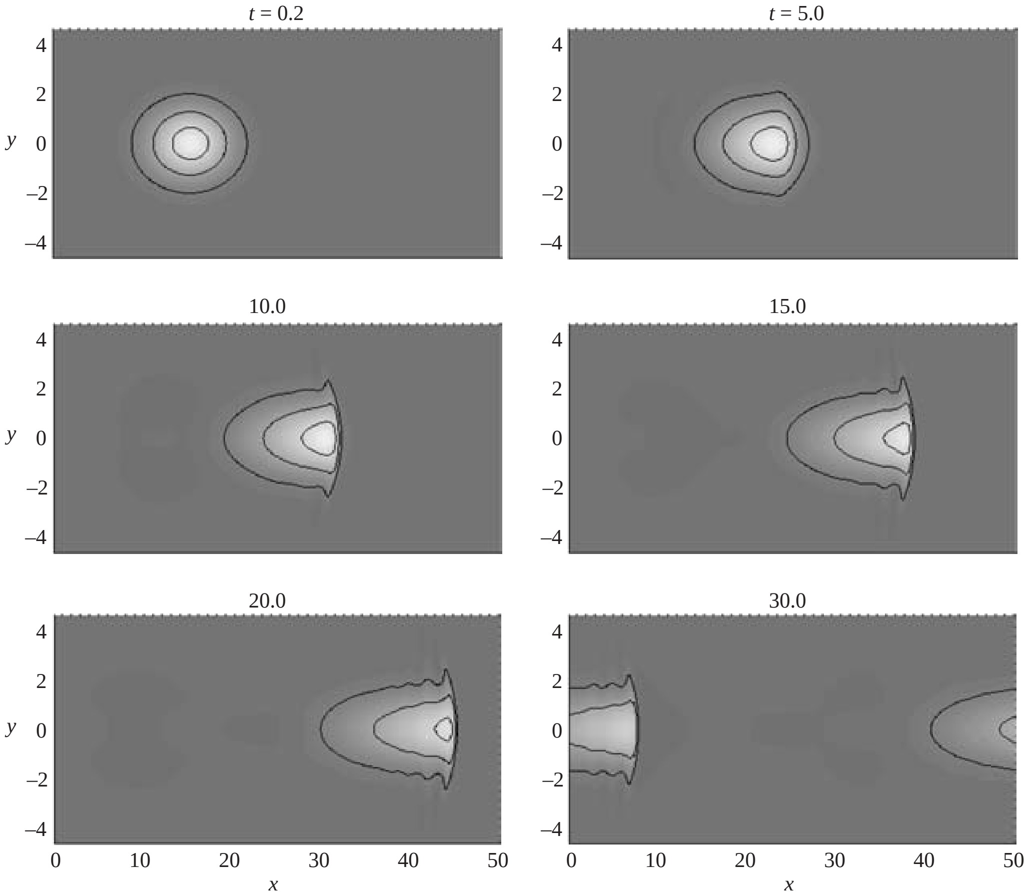

FIGURE 4. Evolution of a nonlinear Kelvin wave with $\delta = 0.3$ and $Ro = 0.5$. The wave breaks in finite time ($\sim 10T$) forming a shock. inertia–gravity wave emission starts at this moment behind the front and continues. The isolines $h = 1.05, 1.2, 1.4$ are shown.

with this estimate. Note that the phase speed of the emitted inertia–gravity waves is roughly the same as the shock speed.

Since nonlinear Kelvin waves of the opposite sign are moving slower than linear ones they should not emit inertia–gravity waves by direct resonance, which we confirm in the corresponding simulation presented in figure 5. The parameters are the same as in figure 4, except for the sign of the perturbation, which is opposite (depression). A conclusion one can draw from the simulation of the Kelvin-wave breaking in the context of adjustment and fast–slow motion interactions is that formation of the Kelvin 'fore-fronts' does produce short-scale inertia–gravity waves (fast motion), while formation of the 'back-fronts' does not. Kelvin fronts are zones of enhanced dissipation and, thus, attenuate the initial disturbance by providing an energy sink complementary to the dissipationless inertia–gravity-wave emission. The amplitude of the jump in h varies along the Kelvin front. Therefore Kelvin fronts change the potential vorticity distribution as they pass (cf. Appendix F). In this way secondary jets are formed behind the Kelvin fronts as shown in figure 6. Thus, the Kelvin-wave breaking does mean an onset of slow–fast motion interactions, as was seen in figure 4. However, its main influence on the slow motion is due to dissipative effects.

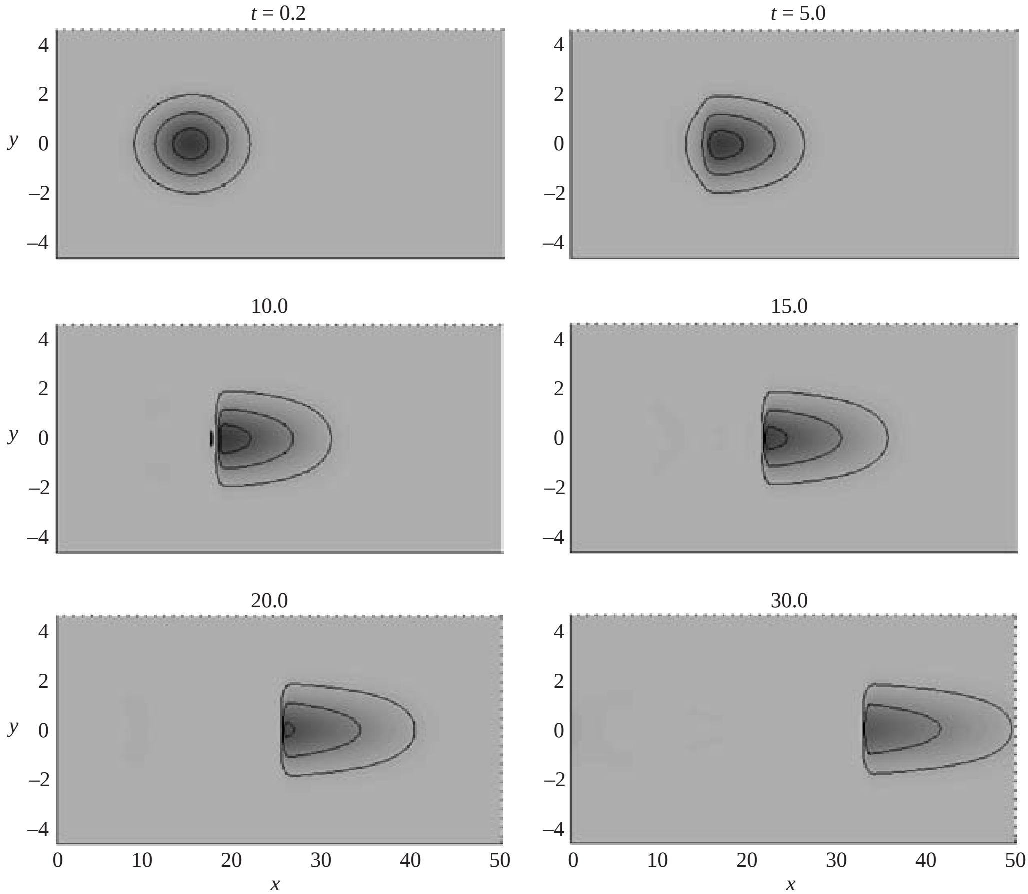

FIGURE 5. Evolution of a nonlinear Kelvin wave with $\delta = 0.3$ and $Ro = -0.5$. The wave breaks in finite time ($\sim 10T$) forming a shock. There is no inertia–gravity wave emission. Contours $h = 0.6, 0.8, 0.95$ are shown.

4.3. *Nonlinear Rossby waves*

We then tested the limits of the fast–slow splitting in the evolution of the Rossby-wave part of the moderately nonlinear perturbation. As initial conditions we took a Gaussian perturbation in the zonal direction with a meridional structure for all fields corresponding to the Rossby wave with $n = 1$. The Rossby number was taken to be 0.35 and the aspect ratio $\delta = 0.1$, i.e. the parameters are well beyond the asymptotic regime where the KdV equation (3.37) is formally valid. The evolution of such a disturbance is presented in figure 7. Surprisingly, this essentially nonlinear perturbation behaves according to the KdV pattern. Recall that within the framework of the KdV equation any localized perturbation undergoes fission into a sequence of solitons of diminishing amplitude (and, correspondingly, diminishing propagation velocity). This is exactly what is observed in figure 7, although the observed modons are strongly nonlinear (a clear criterion of strong nonlinearity is the transport of mass; we call dipolar structures with recirculation mass-trapping zones inside 'modons', otherwise those are 'solitons', although they are not necessarily solutions of the KdV equation at high enough amplitudes). This means that, at least for perturbations

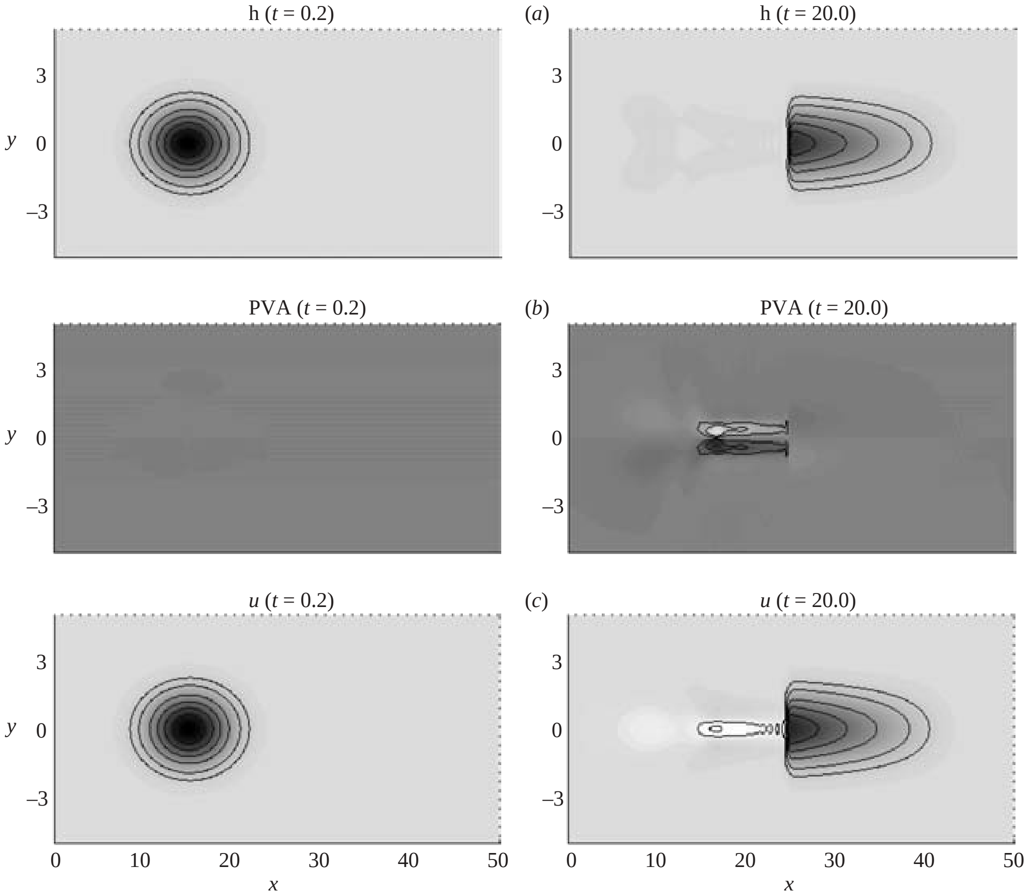

FIGURE 6. (a) Potential vorticity deposit in the wake of a broken Kelvin wave at $Ro = 0.6$. Isolines of h between 0.5 and 1.1 are shown. (b) The PV-anomaly $q = \frac{v_x - u_y + \beta y}{H} - \frac{\beta y}{H_0}$. The isolines of q between −0.2 and 0.2 are shown. (c) the distribution of the u-field.

symmetric in y, the 'breaking' of Rossby waves consists of the formation of a sequence of equatorial modons. Remarkably, each of the structures in the later panels of figure 7 is in the $Ro \sim \delta^2$ regime, although δ is not very small for each of them. It is worth noting that the height anomaly intensifies for the leading modon during this process.

In order to further test the interactions of the westward-propagating slow (Rossby) part of the initial perturbation and inertia–gravity waves we followed the evolution of a 'soliton' (cf. Boyd 1980a) with non-dimensional amplitude $\sim$0.3. A typical evolution of the height field is presented in figure 8. A field of inertia–gravity waves of weak intensity is seen in front of the soliton, while a (mostly Rossby-wave) wake is formed behind. Although the modons or 'solitons' like the one presented on figure 8 are quite stationary, the simulation suggests that they emit inertia–gravity waves, although the precise origin of the observed IGW cannot be determined at this stage. Several mechanisms may be at work, and to distinguish among them further investigation, which is beyond the scope of the present paper, is necessary. As possible explanations we would mention a direct resonance of the soliton with the west-moving inertia–gravity waves (like in the Kelvin front case; however the time-evolution of the field

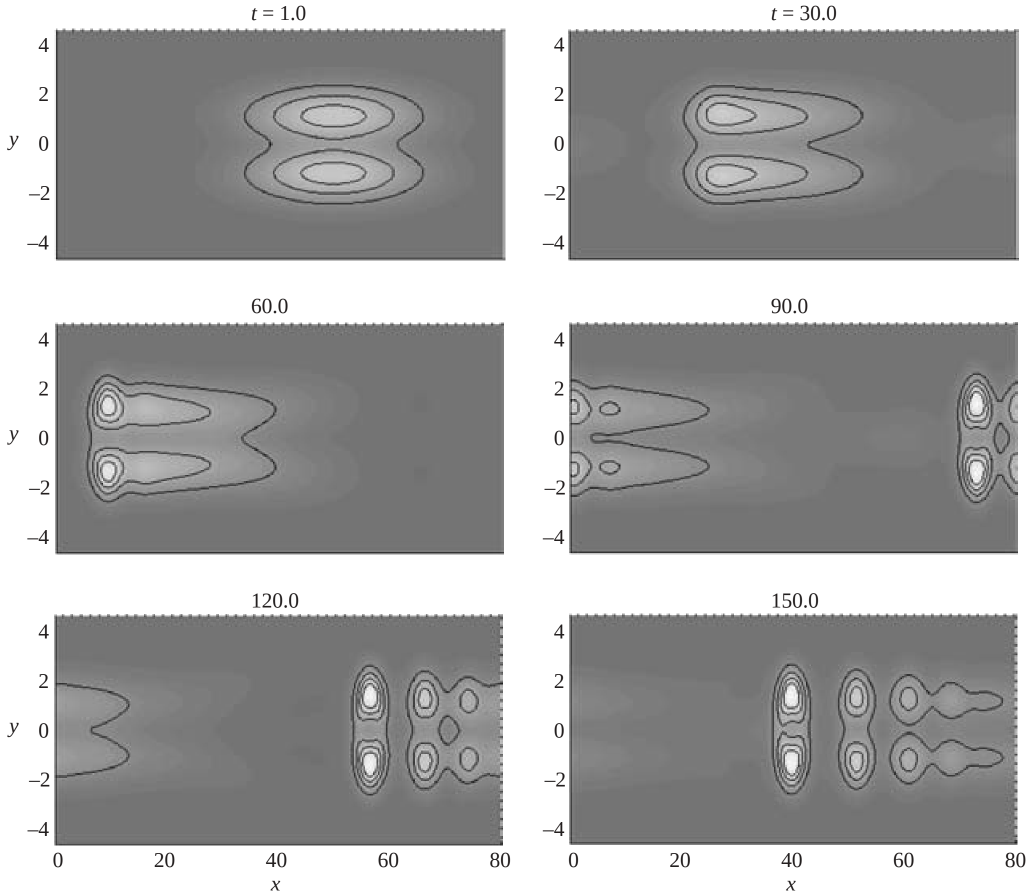

FIGURE 7. Long-time evolution of a nonlinear dipolar perturbation with $\delta = 0.1$, $Ro = 0.35$. The initial perturbation forms a sequence of modons of diminishing amplitude and phase speed. The isolines $h = 1.1, 1.2, 1.3, 1.4$ are shown. Note a build-up in amplitude for the leading modon with respect to the initial perturbation.

presented in figure 8 suggests that it is the group velocity of the inertia–gravity-wave packet which coincides with the speed of the Rossby solitons, while the phase velocity of the inertia–gravity waves is higher), a non-local resonant triad interaction of the type described by Ripa (1983), and a synchronization of IGW produced by adjustment of the initial perturbation as they pass through the modon.

Note that we limited presentation of numerical simulations in this section to those symmetric with respect to equator perturbations. That is, in these simulations we excluded antisymmetric Yanai waves which have the lowest frequency of all fast waves and asymptotics approaching those of (short) Rossby waves at large negative wavenumbers. An exhaustive numerical investigation of equatorial adjustment in strongly nonlinear regimes with special emphasis on wave breaking, which is particularly significant for Yanai waves, will be presented elsewhere. Let us only mention in this context that previous numerical simulations of eccentric pressure perturbations by Fedorov & Melville (2000) confirm our theoretical predictions, which is also the case for our simulations at low Rossby numbers (not presented).

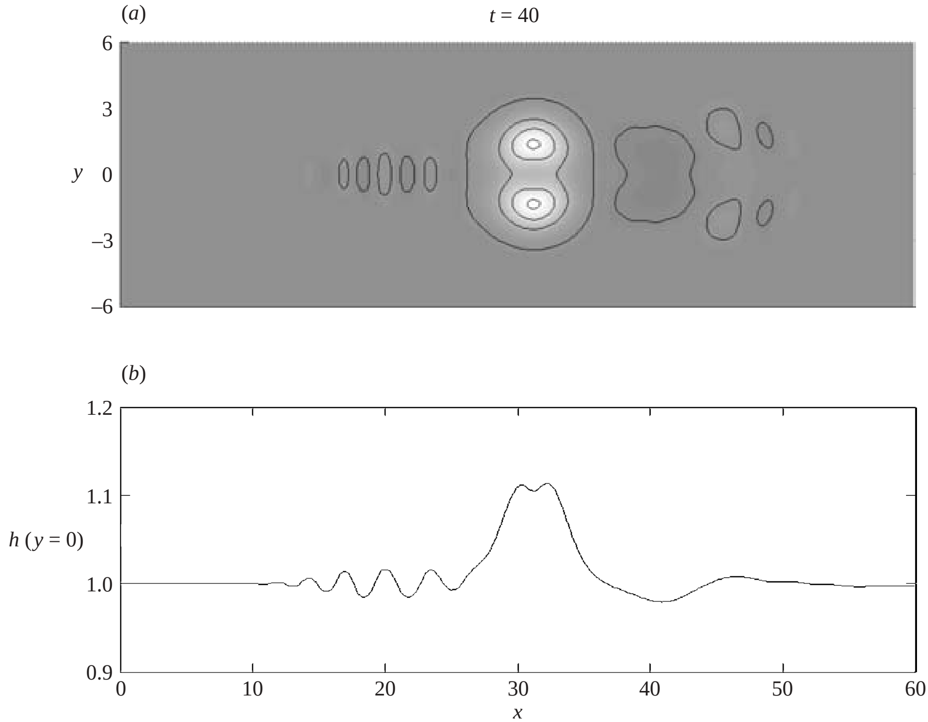

FIGURE 8. (*a*) Inertia–gravity waves and a Rossby-wave soliton with $Ro \sim 0.3$. (*a*) The height field with isolines $h = 0.99, 1.01, 1.1, 1.2, 1.3$ shown. (*b*) An equatorial section of the height field. inertia–gravity waves in front of the (westward-propagating) soliton are clearly seen. Behind the soliton there is a wake of weak Rossby waves

5. Summary and discussion

We have considered the evolution of localized zonally elongated perturbations on the equatorial beta-plane in the framework of the rotating shallow-water model. An inspection of the dispersion curve for linear equatorial waves shows a characteristic spectral gap in the long-wave region between the slow Kelvin and Rossby waves, and the fast Yanai and inertia–gravity waves. An asymptotic multiple-timescale theory we constructed confirms that in the weakly nonlinear regime these slow and fast components of motion are dynamically split, each obeying its own evolution equation while propagating out from the initial disturbance. The absence of the fast-motion drag upon the slow motion is proved by a direct analytic computation. Possible weakly nonlinear regimes are classified with respect to the relation between the Rossby number and the aspect ratio of the perturbation. In a specific regime with Rossby number of the order of the square of the aspect ratio, the westward-propagating Rossby-wave part of the spectrum obeys a KdV evolution equation for its zonal evolution. The eastward-propagating Kelvin-wave part obeys the simple wave equation and inevitably breaks, thus setting limits for the asymptotic theory. To go beyond these limits a high-resolution shock-capturing code was applied to simulate the evolution of essentially nonlinear perturbations numerically. The numerical simulations showed that the breaking does introduce the generation of a wake of inertia–gravity waves behind the Kelvin fore-front, although this wake stays relatively close to the front and does not back-react, for rather long times. Kelvin back-fronts do not generate waves. Kelvin fronts are zones of localized dissipation which modify the distribution of potential vorticity and produce secondary structures in the wake of the front.

We find that essentially nonlinear dipolar perturbations evolve in a striking similar way to the KdV solitons, although they are definitely outside the range of the asymptotic theory which predicts KdV as the evolution equation. Therefore, we deduce that breaking of symmetric (with respect to equator) nonlinear Rossby waves consists of the formation of sequences of modons. Indications of inertia–gravity-wave emission by modons are obtained.

We are grateful to F. Bouchut for providing his numerical code and for numerous helpful discussions of numerical simulations. We thank A. Majda for helpful remarks on the original version of the manuscript and useful discussion.

G.M.R. gratefully acknowledges the kind hospitality of LMD during his stay in Paris. His research was supported by RFBR grant No 020564019. V.Z. acknowledges financial support from the French national program PATOM.

Appendix A. Linear equatorial waves – a reminder

A.1. *Some useful formulae for the parabolic cylinder functions* ϕ_n

$$\phi_n'' + (2n + 1 - y^2)\phi_n = 0, \tag{A 1}$$

$$\phi_n(y) = \frac{H_n(y)\exp(-y^2/2)}{\sqrt{2^n n!\sqrt{\pi}}}, \tag{A 2}$$

where H_n are Hermite polynomials:

$$H_n'(y) = 2nH_{n-1}(y), \ n = 1, 2, \ldots, \tag{A 3}$$

$$H_{n+1}(y) - 2yH_n + 2nH_{n-1}(y) = 0, \quad n = 1, 2, \ldots, \tag{A 4}$$

$$\phi_n' = \frac{\exp(-y^2/2)}{\sqrt{2^n n!\sqrt{\pi}}}\left(nH_{n-1} - \tfrac{1}{2}H_{n+1}\right), \tag{A 5}$$

$$y\phi_n = \frac{\exp(-y^2/2)}{\sqrt{2^n n!\sqrt{\pi}}}\left(nH_{n-1} + \tfrac{1}{2}H_{n+1}\right), \tag{A 6}$$

$$\phi_n' + y\phi_n = \sqrt{2n}\phi_{n-1}, \tag{A 7}$$

$$\phi_n' - y\phi_n = \sqrt{2(n+1)}\phi_{n+1}. \tag{A 8}$$

A.2. *Kelvin wave*

The non-dimensional linear RSW equations are

$$u_t - yv + h_x = 0, \tag{A 9}$$

$$v_t + yu + h_y = 0, \tag{A 10}$$

$$h_t + u_x + v_y = 0. \tag{A 11}$$

By the change of variables (Gill 1980)

$$f = \tfrac{1}{2}(u + h), \quad g = \tfrac{1}{2}(u - h) \tag{A 12}$$

equations (A 9)–(A 11) simplify. They admit a particular solution with $v = 0$ and

$$f = F(x - t, y), \quad g = G(x + t, y). \tag{A 13}$$

For meridionally bounded solutions $G = 0$ and the Kelvin-wave solution is given by

$$u = F_0(x-t)\exp(-y^2/2), \quad h = F_0(x-t)\exp(-y^2/2), \quad v = 0. \tag{A 14}$$

The function F_0 is determined by expanding the initial condition $f_I = \frac{1}{2}(u_I + h_I)$ in a series in parabolic cylinder functions, $f_I = \sum_{n=0}^{\infty} f_{I_n}\phi_n(y)$. Hence, the function F_0 is given by

$$F_0(x) = f_{I_0}(x) = \frac{1}{2}\int_{-\infty}^{+\infty}(u_I + h_I)\phi_0(y)\,\mathrm{d}y \tag{A 15}$$

and the initial conditions for the Kelvin wave are

$$u_I^{(K)} = f_{I_0}\phi_0, \quad h_I^{(K)} = f_{I_0}\phi_0, \quad v_I^{(K)} = 0. \tag{A 16}$$

A.3. *Yanai wave*

The Yanai-wave solution corresponds to $g = 0, f \neq 0, v \neq 0$. In this case from (A 9–A 11) it follows that

$$v = v_0(x,t)\phi_0(y) \tag{A 17}$$

and by expanding the function f in a series in ϕ_n we obtain

$$f = F_1(x,t)\phi_1(y). \tag{A 18}$$

Hence

$$F_{1_t} + F_{1_x} - \frac{1}{\sqrt{2}}v_0 = 0, \quad v_{0_t} + \sqrt{2}F_1 = 0. \tag{A 19}$$

The initial conditions for the Yanai wave are

$$u_I^{(Y)} = \tfrac{1}{2}(u_{I_1} + h_{I_1})\phi_1, \quad h_I^{(Y)} = \tfrac{1}{2}(u_{I_1} + h_{I_1})\phi_1, \quad v_I^{(Y)} = v_{I_0}\phi_0. \tag{A 20}$$

where, as above, we suppose that initial conditions are expanded in ϕ_n. In terms of the variable v the Yanai wave is a solution of the following problem, cf. (A 17)–(A 19), (A 20):

$$v_{tt}^{(Y)} + v_{xt}^{(Y)} + v^{(Y)} = 0, \quad v_I^{(Y)} = v_{I_0}\phi_0, \quad v_t^{(Y)}\big|_{t=0} = -\frac{1}{\sqrt{2}}(u_{I_1} + h_{I_1})\phi_0. \tag{A 21}$$

The solution has the form (A 17) with v_0 given by

$$v_0 = \int \mathrm{d}k \frac{|\sigma_2|\tilde{v}_{I_0} - \mathrm{i}\sqrt{2}\tilde{f}_{I_1}}{\sqrt{k^2+4}}\,\mathrm{e}^{\mathrm{i}(kx-\sigma_1 t)} + \int \mathrm{d}k \frac{\sigma_1\tilde{v}_{I_0} + \mathrm{i}\sqrt{2}\tilde{f}_{I_1}}{\sqrt{k^2+4}}\,\mathrm{e}^{\mathrm{i}(kx+|\sigma_2|t)}, \tag{A 22}$$

where

$$\sigma_1 = \frac{k}{2} + \sqrt{\frac{k^2}{4}+1}, \quad |\sigma_2| = -\frac{k}{2} + \sqrt{\frac{k^2}{4}+1} \tag{A 23}$$

and we defined the Fourier-transforms of the initial fields:

$$v_{I_0}(x) = \int \mathrm{d}k\,\tilde{v}_{I_0}(k)\,\mathrm{e}^{\mathrm{i}kx}, \quad \tfrac{1}{2}(u_{I_1} + h_{I_1}) = \int \mathrm{d}k\,\tilde{f}_{I_1}(k)\,\mathrm{e}^{\mathrm{i}kx}. \tag{A 24}$$

A.4. *Rossby and inertia–gravity waves*

The use of the full equation for the v-field which follows from (A 9)–(A 11) by eliminating u and h is necessary for determining this part of the spectrum:

$$\partial_t\left(\Delta v - y^2 v - \partial_{tt}v\right) + \partial_x v = 0. \tag{A 25}$$

The three initial conditions are

$$\left.\begin{aligned} v|_{t=0} &= v_I^{(RG)}, \\ v_t|_{t=0} &= -\left(y u_I^{(RG)} + h_{I_y}^{(RG)}\right), \\ v_{tt}|_{t=0} &= v_{I_{yy}}^{(RG)} - y^2 v_I^{(RG)} + \partial_x \left(u_{I_y}^{(RG)} + y h_I^{(RG)}\right), \end{aligned}\right\} \tag{A 26}$$

where

$$u_I^{(RG)} = u_I - u_I^{(K)} - u_I^{(Y)} = \tfrac{1}{2}(u_{I_0} - h_{I_0})\phi_0 + \tfrac{1}{2}(u_{I_1} - h_{I_1})\phi_1 + \sum_{n=2}^{\infty} u_{I_n}(x)\phi_n(y) \tag{A 27}$$

$$h_I^{(RG)} = h_I - h_I^{(K)} - h_I^{(Y)} = -\tfrac{1}{2}(u_{I_0} - h_{I_0})\phi_0 - \tfrac{1}{2}(u_{I_1} - h_{I_1})\phi_1 + \sum_{n=2}^{\infty} h_{I_n}(x)\phi_n(y), \tag{A 28}$$

$$v_I^{(RG)} = v_I - v_I^{(Y)} = \sum_{n=1}^{\infty} v_{I_n}(x)\phi_n(y). \tag{A 29}$$

By expanding v in a series in ϕ_n, $v = \sum_n v_n(x,t)\phi_n(y)$, we obtain for v_n

$$\partial_t \left[\partial_{xx}^2 v_n - (2n+1)v_n - \partial_{tt}^2 v_n\right] + \partial_x v_n = 0, \tag{A 30}$$

while for its Fourier-transform $\tilde{v}_n(k,t) = \int \mathrm{d}x\, \mathrm{e}^{-\mathrm{i}kx} v_n(x,t)$ we obtain

$$\partial_{ttt}^3 \tilde{v}_n + (k^2 + 2n + 1)\partial_t \tilde{v}_n - \mathrm{i}k\tilde{v}_n = 0. \tag{A 31}$$

Hence

$$\tilde{v}_n = v_{n_1}(k)\,\mathrm{e}^{-\mathrm{i}\sigma_{n_1} t} + v_{n_2}(k)\,\mathrm{e}^{-\mathrm{i}\sigma_{n_2} t} + v_{n_3}(k)\,\mathrm{e}^{-\mathrm{i}\sigma_{n_3} t} \tag{A 32}$$

where σ_{n_α}, $\alpha = 1, 2, 3$, are the three roots of the dispersion equation

$$\sigma_{n_\alpha}^3 - (k^2 + 2n + 1)\sigma_{n_\alpha} - k = 0. \tag{A 33}$$

By introducing the projections $v_{I_n}, v_{t_{I_n}}, v_{tt_{I_n}}$ of the initial conditions v_I, v_{t_I}, v_{tt_I}, respectively, onto the corresponding ϕ_n, and their Fourier-transforms, we obtain the following system of algebraic equations for $v_{n(\alpha)}$:

$$\sum_{\alpha=1}^{3} v_{n_\alpha} = \tilde{v}_{n_I}, \quad \sum_{\alpha=1}^{3} \sigma_{n_\alpha} v_{n_\alpha} = \mathrm{i}\tilde{v}_{t_{n_I}}, \quad \sum_{\alpha=1}^{3} \sigma_{n_\alpha}^2 v_{n_\alpha} = -\tilde{v}_{tt_{n_I}}. \tag{A 34}$$

The lowest eigenvalue σ_1 defines the Rossby mode, the other two the inertia–gravity wave modes. For the Rossby mode we obtain

$$v_1^{(1)} = \frac{1}{2\sigma_{n_1}^3}\left(k\tilde{v}_{n_I} + \mathrm{i}\sigma_{n_1}^2 \tilde{v}_{t_{n_I}} - \sigma_{n_1}\tilde{v}_{tt_{n_I}}\right). \tag{A 35}$$

Therefore, the part of the initial conditions corresponding to this wave may be determined, and similarly for the gravity-wave modes.

Appendix B. Long Kelvin waves in the presence of the mean zonal flow

In the absence of the zonal flow the non-dispersive Kelvin waves always overturn due to advective nonlinearity. If the balanced mean flow $u^{(M)}(y)$, $h^{(M)}(y)$ with

$$y u^{(M)}(y) + h^{(M)}(y) = 0 \tag{B 1}$$

is present, it may prevent breaking of Kelvin waves. In the presence of the mean flow equations (2.10)–(2.11) take the form

$$u_{t_1} + \epsilon_1\big(u^{(M)}u_x + vu_y^{(M)}\big) + \epsilon(uu_x + vu_y) - yv = -h_x, \quad \text{(B 2)}$$

$$\delta^2 v_{t_1} + \delta^2\epsilon_1 u^{(M)}v_x + \delta^2\epsilon(uv_x + \epsilon vv_y) + yu = -h_y, \quad \text{(B 3)}$$

$$h_{t_1} + v_y + u_x + \epsilon_1\big[\big(h^{(M)}v\big)_y + \big(h^{(M)}u + hu^{(M)}\big)_x\big] + \epsilon\big[(hv)_y + (hu)_x\big] = 0. \quad \text{(B 4)}$$

Here the Rossby numbers ϵ_1 and ϵ are related to the mean flow and Kelvin waves, respectively. Both ϵ_1 and ϵ are assumed small. We would like to find a relation between ϵ_1 and ϵ allowing the breaking of Kelvin waves to be prevented.

At the lowest order in Rossby numbers we have (2.13)–(2.15) and for the Kelvin waves

$$v^{(0)} = 0 \Rightarrow u^{(0)} = h^{(0)} = U_0(x - t_1, t_2)\,\phi_0(y). \quad \text{(B 5)}$$

The next terms of the perturbation theory are of order $\max(\epsilon, \epsilon_1)$ and we find

$$u_{t_1}^{(1)} - yv^{(1)} + h_x^{(1)} = -u_{t_2}^{(0)} - \frac{\epsilon_1}{\max(\epsilon,\epsilon_1)}u^{(M)}u_x^{(0)} - \frac{\epsilon}{\max(\epsilon,\epsilon_1)}u^{(0)}u_x^{(0)}, \quad \text{(B 6)}$$

$$yu^{(1)} + h_y^{(1)} = 0, \quad \text{(B 7)}$$

$$h_{t_1}^{(1)} + u_x^{(1)} + v_y^{(1)} = -h_{t_2}^{(0)} - \frac{\epsilon}{\max(\epsilon,\epsilon_1)}\big(h^{(0)}u^{(0)}\big)_x + \frac{\epsilon_1}{\max(\epsilon,\epsilon_1)}\big(h^{(0)}u^{(M)} + u^{(0)}h^{(M)}\big)_x. \quad \text{(B 8)}$$

Introducing the notation $R_u^{(1)}, R_h^{(1)}$ for the right-hand side of (B 6) and (B 8), respectively, we obtain after simple manipulations a single equation for $v^{(1)}$ from (B 6)–(B 8):

$$\big(v_{yy}^{(1)} - y^2v^{(1)}\big)_{t_1} + v_x^{(1)} = -\big[\big(R_u^{(1)} + R_h^{(1)}\big)_y + y\big(R_u^{(1)} + R_h^{(1)}\big)\big] = R_v^{(1)}. \quad \text{(B 9)}$$

The forcing on the right-hand side of (B 9) is defined from the zero-order Kelvin-wave solution (B 5) and has the form $R_v^{(1)} = R_v^{(1)}(x - t_1, y)$. Therefore, the forced solution of (B 9) is

$$v^{(1)} = v^{(1)}(x - t_1, y). \quad \text{(B 10)}$$

From (B 6), (B 8) we obtain

$$\big(u^{(1)} + h^{(1)}\big)_{t_1} + \big(u^{(1)} + h^{(1)}\big)_x + v_y^{(1)} - yv^{(1)} = R_u^{(1)} + R_h^{(1)}. \quad \text{(B 11)}$$

The resonant terms are absent in (B 11) if

$$v_y^{(1)} - yv^{(1)} = R_u^{(1)} + R_h^{(1)}. \quad \text{(B 12)}$$

Equation (B 12) has a solution bounded in y if

$$\int_{-\infty}^{+\infty}\big(R_u^{(1)} + R_h^{(1)}\big)\phi_0(y)\,\mathrm{d}y = 0 \quad \text{(B 13)}$$

which defines the slow-time evolution of Kelvin waves. A simple analysis shows that when the mean flow is weak, $\epsilon \geqslant \epsilon_1$, the slow evolution is given by the simple wave equation. Breaking takes place at finite time, and the phase velocity of the wave acquires a correction to the phase speed due to the mean flow. Dispersion does not occur in this regime. Hence, in order to prevent breaking we need $\epsilon \ll \epsilon_1$. In order to determine the precise relation between ϵ and ϵ_1 that stops the nonlinear breaking of the Kelvin wave by dispersion, it is worth noting that dispersion in the system is entirely due to the term $\delta^2 v_{t_1}$ in (B 3) and that the evolution takes place on the timescale t_2, the next slow time with respect to t_1. Under condition $\epsilon \ll \epsilon_1$ this timescale is $t_2 = \epsilon_1 t_1$ independently of the value of δ (the correction to the phase-speed due to the mean flow appears precisely at this timescale). As the order of magnitude of v_{t_2} is $O(\epsilon_1^2)$ (because of $v^{(1)} \sim \epsilon_1$), the dispersive term $\delta^2 v_{t_2} \sim \delta^2 \epsilon_1^2$ and the nonlinearity have to appear at the same order. Therefore, we arrive to the conclusion that a mean flow may prevent Kelvin wave breaking only if

$$\delta^2 \epsilon_1^2 \sim \epsilon, \tag{B 14}$$

i.e. for a rather small amplitude of the Kelvin wave. If the mean flow and the wave have the same amplitude, $\epsilon \sim \epsilon_1$, as in the main body of the paper, Kelvin waves break.

Appendix C. Details of calculations for $Ro = O(\delta^2)$ adjustment

C.1. δ^0-approximation

As follows from (3.9), (3.10), (3.15), and (3.16)

$$\bar{v}^{(0)} = 0, \tag{C 1}$$

$$y\bar{u}^{(0)} + \bar{h}_y^{(0)} = 0. \tag{C 2}$$

Equation (3.27) for the fast fields is written as

$$\tilde{v}_{tt}^{(0)} - \tilde{v}_{yy}^{(0)} + y^2 \tilde{v}^{(0)} = 0. \tag{C 3}$$

Its solution has the form

$$\tilde{v}^{(0)} = \sum_{n=0}^{\infty} \tilde{v}_n^{(0)}(x, t)\phi_n(y), \tag{C 4}$$

where

$$\tilde{v}_n^{(0)} = A_{0_n}^{+}(x, t_1, t_2, \ldots)\mathrm{e}^{\mathrm{i}\sigma_n t} + A_{0_n}^{-}(x, t_1, t_2, \ldots)\mathrm{e}^{-\mathrm{i}\sigma_n t}, \quad \sigma_n = \sqrt{2n+1}. \tag{C 5}$$

The initial conditions for all fields are uniquely defined – see Appendix D. Thus, we have a yet undefined geostrophically balanced slow field (C 1), (C 2) and a spectrum of fast Yanai ($n = 0$) and inertia–gravity waves ($n > 0$).

It is convenient to introduce the primitive of the fast meridional velocity with zero mean:

$$\tilde{V}_0 = \int \mathrm{d}t\ \tilde{v}^{(0)} = -\sum_{n=0}^{\infty} \frac{\tilde{v}_{n_t}^{(0)}(x, t)}{\sigma_n^2}\phi_n(y), \quad \overline{\tilde{V}}_0 = 0. \tag{C 6}$$

Correspondingly, from (3.19), (3.21):

$$\tilde{u}^{(0)} = y\tilde{V}_0 = -y\sum_{n=0}^{\infty} \frac{\tilde{v}_{n_t}^{(0)}(x, t)}{\sigma_n^2}\phi_n(y), \quad \tilde{h}^{(0)} = -\tilde{V}_{0_y} = \sum_{n=0}^{\infty} \frac{\tilde{v}_{n_t}^{(0)}(x, t)}{\sigma_n^2}\phi_{n_y}(y). \tag{C 7}$$

C.2. δ^1-approximation

C.2.1. *Slow component*

By virtue of (3.22) for $n = 1$, (3.11), and (C 1) we have the following equation for $\bar{v}^{(1)}$:

$$\left(\bar{v}_{yy}^{(1)} - y^2 \bar{v}^{(1)}\right)_{t_1} + \bar{v}_x^{(1)} = 0, \tag{C 8}$$

with a solution

$$\bar{v}^{(1)} = \sum_{n=0}^{\infty} \bar{v}_n^{(1)}(x + \bar{c}_n t_1)\phi_n(y). \tag{C 9}$$

The first term of the expansion, $\bar{v}_0^{(1)}(x + t_1)\phi_0(y)$, is of Yanai-wave form. We show in Appendix D that $\bar{v}_0^{(1)} = 0$. Once $\bar{v}^{(1)}$ is known, $\bar{u}^{(0)}$ and $\bar{h}^{(0)}$ may be found. By introducing (cf. (A 12)) the functions

$$\bar{f}^{(0)} = \bar{u}^{(0)} + \bar{h}^{(0)}, \quad \bar{g}^{(0)} = \bar{u}^{(0)} - \bar{h}^{(0)} \tag{C 10}$$

we obtain from (3.15) and (3.17) for $n = 1$

$$\bar{f}_{t_1}^{(0)} + \bar{f}_x^{(0)} = y\bar{v}^{(1)} - \bar{v}_{1_y}^{(1)}, \quad \bar{g}_{t_1}^{(0)} - \bar{g}_x^{(0)} = \bar{v}_y^{(1)} + y\bar{v}^{(1)}. \tag{C 11}$$

The full solution of these equations is

$$\bar{f}^{(0)} = F_0(x - t_1, y) + \bar{\mathscr{F}}_0, \quad \bar{g}^{(0)} = G_0(x + t_1, y) + \bar{\mathscr{G}}_0, \tag{C 12}$$

where F_0, G_0 are yet undetermined solutions of the corresponding homogeneous equations and $\bar{\mathscr{F}}_0, \bar{\mathscr{G}}_0$ are the forced solutions of the form

$$\bar{\mathscr{F}}_0 = \sum_{n=1}^{\infty} \frac{\sqrt{2(n+1)}}{1+\bar{c}_n} \bar{\mathscr{V}}_{1_n}(x + \bar{c}_n t_1)\,\phi_{n+1}(y), \tag{C 13}$$

$$\bar{\mathscr{G}}_0 = \sum_{n=1}^{\infty} \frac{\sqrt{2n}}{1-\bar{c}_n} \bar{\mathscr{V}}_{1_n}(x + \bar{c}_n t_1)\,\phi_{n-1}(y). \tag{C 14}$$

When deriving these expressions, we substituted (C 9) into (C 11) and used (A 7), (A 8). The functions $\bar{\mathscr{V}}_{1_n}$ are the primitives of $\bar{v}_n^{(1)}$ with respect to x: $\bar{\mathscr{V}}_{1_{n_x}} = \bar{v}_n^{(1)}$, and may be determined from the initial conditions, cf. (D 21) in Appendix D:

$$\bar{\mathscr{V}}_{1_n}(x) = \left(\bar{u}_{I_{n+1}}^{(0)}(x) + \bar{h}_{I_{n+1}}^{(0)}(x)\right) \frac{\sqrt{2(n+1)}}{2n+1}. \tag{C 15}$$

The functions F_0, G_0, too, may be determined from initial conditions (cf. Appendix D). In terms of initial variables we obtain

$$\bar{u}^{(0)}(x, y, t_1) = U_0(x - t_1)\phi_0(y) + \tfrac{1}{2}(\bar{\mathscr{F}}_0 + \bar{\mathscr{G}}_0), \tag{C 16}$$

$$\bar{h}^{(0)}(x, y, t_1) = U_0(x - t_1)\phi_0(y) + \tfrac{1}{2}(\bar{\mathscr{F}}_0 - \bar{\mathscr{G}}_0), \tag{C 17}$$

with

$$U_0(x) = \bar{u}_{I_0}^{(0)}(x) + \bar{h}_{I_0}^{(0)}(x). \tag{C 18}$$

The full slow solution $(\bar{u}^{(0)}, \bar{v}^{(1)}, \bar{h}^{(0)})$ is a sum of three contributions (3.32), (3.33)–(3.35), and (3.36). All of them are unambiguously defined.

C.2.2. *Fast component*

By virtue of (3.11) and (3.27) for $n = 1$ we have for $\tilde{v}^{(1)}$

$$\tilde{v}_{tt}^{(1)} + y^2\tilde{v}^{(1)} - \tilde{v}_{yy}^{(1)} = -2\tilde{v}_{tt_1}^{(0)} + \tilde{V}_{0_x}. \tag{C 19}$$

The right-hand side of (C 19) is resonant and, hence, should vanish:

$$-2\tilde{v}_{tt_1}^{(0)} + \tilde{V}_{0_x} = 0 \;\Rightarrow -2\tilde{v}_{ttt_1}^{(0)} + \tilde{v}_x^{(0)} = 0. \tag{C 20}$$

Expanding this expression in $\phi_n(y)$ we find the equation

$$A^{\pm}_{0_n}(x, t_1) = A^{\pm}_{0_n}\left(x - \frac{t_1}{2\sigma_n^2}\right) \tag{C 21}$$

which determines the slow-time evolution of the zero-order fast fields. For the first-order fast fields, due to (C 20) equation (C 19) becomes homogeneous and is solved by $\tilde{v}^{(1)} = \sum_{n=0}^{\infty} \tilde{v}_n^{(1)}(x, t, t_1, \ldots)\phi_n(y)$ with

$$\tilde{v}_n^{(1)} = A^{+}_{1_n}(x, t_1, \ldots)\mathrm{e}^{\mathrm{i}\sigma_n t} + A^{-}_{1_n}(x, t_1, \ldots)\mathrm{e}^{-\mathrm{i}\sigma_n t}. \tag{C 22}$$

$\tilde{u}^{(1)}$ and $\tilde{h}^{(1)}$ are determined from (3.19), (3.21) for $n = 1$, and (C 7):

$$\tilde{u}^{(1)} = y\tilde{V}_1 + \tilde{W}_{0_{xy}} - y\tilde{W}_{0_{t_1}}, \tag{C 23}$$

$$\tilde{h}^{(1)} = -\tilde{V}_{1_y} + \tilde{W}_{0_{xt_1}} - y\tilde{W}_{0_x}, \tag{C 24}$$

where $\tilde{V}_1 = \int \mathrm{d}t\, \tilde{v}^{(1)}$ and $\tilde{W}_0 = \int \mathrm{d}t\, \tilde{V}_0$, respectively:

$$\tilde{V}_1(x, y, t) = -\sum_{n=0}^{\infty} \frac{1}{\sigma_n^2}\tilde{v}_{n_t}^{(1)}(x, t, t_1)\phi_n(y), \quad \tilde{W}_0 = -\sum_{n=0}^{\infty} \frac{1}{\sigma_n^2}\tilde{v}_n^{(0)}(x, t, t_1)\phi_n(y). \tag{C 25}$$

C.3. δ^2- *approximation*

C.3.1. *Slow motion*

Using (3.11) and (3.12) we obtain from (3.22) for $n = 2$

$$\left(\bar{v}_{yy}^{(2)} - y^2\bar{v}^{(2)}\right)_{t_1} + \bar{v}_x^{(2)} = \left(y\bar{P}_u^{(2)} + \bar{P}_{h_y}^{(2)}\right)_{t_1} - \left(\bar{P}_{u_y}^{(2)} + y\bar{P}_h^{(2)}\right)_x, \tag{C 26}$$

where

$$\bar{P}_u^{(2)} = -\bar{u}_{t_2}^{(0)} - \overline{\tilde{v}^{(0)}\tilde{u}_y^{(0)}}, \tag{C 27}$$

$$\bar{P}_h^{(2)} = -\bar{h}_{t_2}^{(0)} - \overline{(\tilde{h}^{(0)}\tilde{v}^{(0)})}_y. \tag{C 28}$$

Let us calculate the time-averages entering these equations. Due to (C 5)

$$\overline{\tilde{v}_n^{(0)}\tilde{v}_{m_t}^{(0)}} = \overline{\tilde{v}_n^{(0)}\tilde{v}_m^{(0)}} = 0, \quad m \neq n, \tag{C 29}$$

and, hence, from (C 4), (C 7) we find

$$\overline{\tilde{v}^{(0)}\tilde{u}_y^{(0)}} = -\sum_{n=0}^{\infty} \frac{\overline{\tilde{v}_n^{(0)}\tilde{v}_{n_t}^{(0)}}}{\sigma_n^2}\phi_n(y)(y\phi_n(y))_y = 0, \tag{C 30}$$

$$\overline{\tilde{h}^{(0)}\tilde{v}^{(0)}} = -\sum_{n=0}^{\infty} \frac{\overline{\tilde{v}_n^{(0)}\tilde{v}_{n_t}^{(0)}}}{\sigma_n^2}\phi_n(y)\phi_n(y)_y = 0. \tag{C 31}$$

Using (C 2) one may show that the right-hand side of (C 26) is equal to $(\bar{u}_y^{(0)} + y\bar{h}^{(0)})_{xt_2}$. By differentiating (C 26) in t_1 and using (D 15) we arrive to the following inhomogeneous linear PDE:

$$\hat{L}\bar{v}_{t_1}^{(2)} = \bar{v}_{xt_2}^{(1)} \tag{C 32}$$

where the operator $\hat{L}$ is defined as

$$\hat{L} = \left(\partial_{yy}^2 - y^2\right)\partial_{t_1} + \partial_x. \tag{C 33}$$

The necessary condition for the absence of resonances in (C 32) is $\bar{v}_{t_2}^{(1)} = 0$, which means that $\bar{v}^{(1)}$ and, hence $\bar{u}^{(0)}$ and $\bar{h}^{(0)}$ as well, do not depend on t_2, i.e. the

Rossby-wave part is t_2-independent. Therefore, only the Kelvin-wave part occurs in the right-hand side of (3.15), (3.17) for $n = 1$. By adding these two equations we obtain

$$\left(\bar{u}^{(1)} + \bar{h}^{(1)}\right)_{t_1} + \left(\bar{u}^{(1)} + \bar{h}^{(1)}\right)_x = -\left(\bar{u}^{(0)}_{(K)} + \bar{h}^{(0)}_{(K)}\right)_{t_2} - \left(\bar{v}^{(2)}_y - y\bar{v}^{(2)}\right), \qquad \text{(C 34)}$$

whence it follows that the Kelvin-wave part does not depend on t_2 either, because $\bar{v}^{(2)}$ which satisfies the homogeneous equation (C 32) does not contain terms depending on $x - t_1$. Hence, the second-order slow-component equations (3.15)–(3.17) are homogeneous and are analysed in the same way as in the case $n = 1$.

C.3.2. *Fast motion*

Using (3.12), (3.19)–(3.21) for $n = 0, 1$, equation (3.27) for $\tilde{v}^{(2)}$ takes the form

$$\tilde{v}^{(2)}_{tt} + y^2\tilde{v}^{(2)} - \tilde{v}^{(2)}_{yy} = -2\tilde{v}^{(1)}_{tt_1} + \tilde{V}_{1_x} - 2\tilde{v}^{(0)}_{tt_2} - \tilde{v}^{(0)}_{t_1t_1} + \tilde{v}^{(0)}_{xx} - \tilde{W}_{0xt_1} + y\bar{u}^{(0)}_y\tilde{v}^{(0)} + \left(\bar{h}^{(0)}\tilde{v}^{(0)}\right)_{yy} + R_{NL}, \qquad \text{(C 35)}$$

where the nonlinear part

$$R_{NL} = y\tilde{v}^{(0)}\tilde{u}^{(0)}_y + \left(\tilde{h}^{(0)}\tilde{v}^{(0)}\right)_{yy} - \left(\tilde{v}^{(0)}\tilde{v}^{(0)}_y\right)_t \qquad \text{(C 36)}$$

does not contain any resonances. The linear part does, and hence

$$-2\tilde{v}^{(1)}_{tt_1} + \tilde{V}_{1_x} - 2\tilde{v}^{(0)}_{tt_2} - \tilde{v}^{(0)}_{t_1t_1} + \tilde{v}^{(0)}_{xx} - \tilde{W}_{0xt_1} + \left[y\bar{u}^{(0)}_y\tilde{v}^{(0)} + \left(\bar{h}^{(0)}\tilde{v}^{(0)}\right)_{yy}\right]_{res} = 0, \qquad \text{(C 37)}$$

where the index *res* means resonant part.

The next step consists of considering (C 37) as an equation for $\tilde{v}^{(1)}$ and eliminating resonances at the next timescale t_1. Among the terms not containing $\tilde{v}^{(0)}$, the first four are always resonant, while the last is resonant only if the mean flow $\bar{u}^{(0)}_{(M)}, \bar{h}^{(0)}_{(M)}$ is present. Let us calculate the term $[\ldots]_{res}$ in (C 37). The expansion of the expression inside the square brackets in ϕ_n gives

$$y\bar{u}^{(0)}_y\tilde{v}^{(0)} + \left(\bar{h}^{(0)}\tilde{v}^{(0)}\right)_{yy} = \sum_{n,m} \tilde{v}^{(0)}_m \Phi_{mn}\phi_n, \qquad \text{(C 38)}$$

where

$$\Phi_{mn} = \int_{-\infty}^{+\infty} \mathrm{d}y \left[\bar{h}^{(0)}(y^2 - 2n - 1) + y\bar{u}^{(0)}_y\right]\phi_m\phi_n. \qquad \text{(C 39)}$$

It is easy to see that the resonant part of (C 38) is

$$\left[y\bar{u}^{(0)}_y\tilde{v}^{(0)} + \left(\bar{h}^{(0)}\tilde{v}^{(0)}\right)_{yy}\right]_{res} = \sum_{n} \tilde{v}^{(0)}_n \Phi_{nn}\phi_n. \qquad \text{(C 40)}$$

Decomposing the slow fields into mean-flow, Kelvin-wave and Rossby-wave contributions:

$$\bar{h}^{(0)} = \bar{h}^{(0)}_{(M)}(y) + U_0(x - t_1)\phi_0(y) + \bar{h}^{(0)}_{(R)}, \qquad \text{(C 41)}$$

$$\bar{u}^{(0)} = \bar{u}^{(0)}_{(M)}(y) + U_0(x - t_1)\phi_0(y) + \bar{u}^{(0)}_{(R)}, \qquad \text{(C 42)}$$

we obtain $\Phi_{nn} = \Phi_{nn}^{(M)} + \Phi_{nn}^{(K)} + \Phi_{nn}^{(R)}$, where

$$\Phi_{nn}^{(M)} = \int_{-\infty}^{+\infty} \mathrm{d}y \, \left[\bar{h}_{(M)}^{(0)}(y^2 - 2n - 1) + y\bar{u}_{(M)}^{(0)}\right]\phi_n^2, \tag{C 43}$$

$$\Phi_{nn}^{(K)} = U_0(x - t_1) \int_{-\infty}^{+\infty} \mathrm{d}y \, [\phi_0(y^2 - 2n - 1) + y\phi_{0_y}]\phi_n^2, \tag{C 44}$$

$$\Phi_{nn}^{(R)} = \frac{1}{2}\sum_{m=1}^{\infty} \bar{\mathscr{V}}_{1_m}(x + \bar{c}_m t_1) \int_{-\infty}^{+\infty} \mathrm{d}y \, [P_m^-(y^2 - 2n - 1) + yP_{m_y}^+]\phi_n^2. \tag{C 45}$$

In the last expression the following notation is introduced:

$$P_m^{\pm} = \frac{\sqrt{2(m+1)}}{1 + \bar{c}_m}\phi_{m+1} \pm \frac{\sqrt{2m}}{1 - \bar{c}_m}\phi_{m-1}. \tag{C 46}$$

The only resonant contribution in time t_1 comes from the mean-flow part, and hence the modulation of the zeroth-order fast meridional velocity field $\tilde{v}^{(0)}$ in time t_2 is given by the following equation:

$$2\tilde{v}_{tt_2}^{(0)} + \tilde{v}_{t_1t_1}^{(0)} - \tilde{v}_{xx}^{(0)} + \tilde{W}_{0xt_1} - \sum_n \tilde{v}_n^{(0)}\Phi_{nn}^{(M)}\phi_n = 0. \tag{C 47}$$

Correspondingly, the slow evolution of the first correction $\tilde{v}^{(1)}$ in t_1 is given by

$$2\tilde{V}_{1_{ttt_1}} - \tilde{V}_{1_x} = \sum_n \tilde{v}_n^{(0)}(\Phi_{nn}^{(K)} + \Phi_{nn}^{(R)})\phi_n. \tag{C 48}$$

Substituting (C 4) into (C 47) and taking into account (C 21) we obtain the modulation equation (3.30) for the zero-order wave amplitudes. Substitution of (C 25) and (C 4) into (C 48) gives the equation (3.31) for the first correction to the amplitude.

C.4. δ^3- *approximation*

We will limit consideration to the slow motions which are described by

$$\bar{u}_{t_1}^{(2)} - y\bar{v}^{(3)} + \bar{h}_x^{(2)} = \bar{P}_u^{(3)}, \tag{C 49}$$

$$y\bar{u}^{(2)} + \bar{h}_y^{(2)} = \bar{P}_v^{(2)}, \tag{C 50}$$

$$\bar{h}_{t_1}^{(2)} + \bar{u}_x^{(2)} + \bar{v}_y^{(3)} = \bar{P}_h^{(3)}, \tag{C 51}$$

with

$$\bar{P}_u^{(3)} = -\left(\bar{u}_{t_3}^{(0)} + \bar{u}_{t_2}^{(1)} + \bar{u}^{(0)}\bar{u}_x^{(0)} + \bar{v}^{(1)}\bar{u}_y^{(0)} + \overline{\tilde{v}^{(0)}\tilde{u}_y^{(1)} + \tilde{v}^{(1)}\tilde{u}_y^{(0)}} + \overline{\tilde{u}^{(0)}\tilde{u}_x^{(0)}}\right), \tag{C 52}$$

$$\bar{P}_v^{(2)} = -\left(\bar{v}_{t_1}^{(1)} + \overline{\tilde{v}^{(0)}\tilde{v}_y^{(0)}}\right), \tag{C 53}$$

$$\bar{P}_h^{(3)} = -\left(\bar{h}_{t_3}^{(0)} + \bar{h}_{t_2}^{(1)} + \left(\bar{h}^{(0)}\bar{u}^{(0)}\right)_x + \left(\bar{h}^{(0)}\bar{v}^{(1)}\right)_y + \left(\overline{\tilde{h}^{(1)}\tilde{v}^{(0)} + \tilde{h}^{(0)}\tilde{v}^{(1)}}\right)_y + \left(\overline{\tilde{h}^{(0)}\tilde{u}^{(0)}}\right)_x\right). \tag{C 54}$$

From (C 49) and (C 51) we obtain an equation for $\bar{v}^{(3)}$ (see the definition of $\hat{L}$ in (C 33)):

$$\hat{L}\bar{v}^{(3)} = \left(\frac{\partial^2}{\partial x^2} - \frac{\partial^2}{\partial t_1^2}\right)\left(y\bar{u}^{(2)} + \bar{h}_y^{(2)}\right) + \left(y\bar{P}_u^{(3)} + \bar{P}_{h_y}^{(3)}\right)_{t_1} - \left(\bar{P}_{u_y}^{(3)} + y\bar{P}_h^{(3)}\right)_x, \tag{C 55}$$

which, taking into account (C 50), (C 53) may be rewritten in the form

$$\hat{L}\bar{v}^{(3)} = -\left(\frac{\partial^2}{\partial x^2} - \frac{\partial^2}{\partial t_1^2}\right)\left(\bar{v}_{t_1}^{(1)} + \overline{\tilde{v}^{(0)}\tilde{v}_y^{(0)}}\right) + \left(y\bar{P}_u^{(3)} + \bar{P}_{h_y}^{(3)}\right)_{t_1} - \left(\bar{P}_{u_y}^{(3)} + y\bar{P}_h^{(3)}\right)_x \tag{C 56}$$

Analysis of possible resonances on the right-hand side of (C 56) shows that those due to the stresses of the fast fields are absent (cf. Appendix E). This result is non-trivial because, as follows from (3.31), the variable $\tilde{v}^{(1)}$ does depend parametrically on the slow Rossby waves via the factor $\Phi_{nn}^{(K)} + \Phi_{nn}^{(R)}$. However, this dependence surprisingly drops out from the averages determining the right-hand side of (C 55). Correspondingly, to study the resonant terms in (C 55) it is sufficient to use the truncated expression for the right-hand side:

$$-\left(\frac{\partial^2}{\partial x^2} - \frac{\partial^2}{\partial t_1^2}\right)\bar{v}_{t_1}^{(1)} + \left(y\bar{P}_u^{(3)} + \bar{P}_{h_y}^{(3)}\right)_{t_1} - \left(\bar{P}_{u_y}^{(3)} + y\bar{P}_h^{(3)}\right)_x, \qquad \text{(C 57)}$$

where now

$$\bar{P}_u^{(3)} = -\left(\bar{u}_{t_3}^{(0)} + \bar{u}_{t_2}^{(1)} + \bar{u}^{(0)}\bar{u}_x^{(0)} + \bar{v}^{(1)}\bar{u}_y^{(0)}\right), \qquad \text{(C 58)}$$

$$\bar{P}_h^{(3)} = -\left(\bar{h}_{t_3}^{(0)} + \bar{h}_{t_2}^{(1)} + \left(\bar{h}^{(0)}\bar{u}^{(0)}\right)_x + \left(\bar{v}^{(1)}\bar{h}^{(0)}\right)_y\right). \qquad \text{(C 59)}$$

Expression (C 57) may be written in a more compact form by using the primitives of the variables $\bar{v}^{(1)}$, $\bar{v}^{(2)}$ with respect to the first slow time t_1:

$$\bar{V}_{1_{t_1}} = \bar{v}^{(1)}, \quad \bar{V}_{2_{t_1}} = \bar{v}^{(2)}. \qquad \text{(C 60)}$$

From (D 15) and (3.15), (3.17), (3.18) for $n = 2$, respectively, we have

$$\bar{u}_y^{(0)} + y\bar{h}^{(0)} = \bar{V}_1, \qquad \text{(C 61)}$$

$$\bar{u}_y^{(1)} + y\bar{h}^{(1)} = \bar{V}_2. \qquad \text{(C 62)}$$

Using (C 2), (3.18) for $n = 2$, (D 15) and the fact that $\bar{v}^{(1)}$ does not depend on t_2 and, hence, $\bar{u}^{(0)}, \bar{h}^{(0)}$ do not depend on t_2 either, we obtain the following expression for (C 57):

$$\left(\frac{\partial^2}{\partial x^2} - \frac{\partial^2}{\partial t_1^2}\right)\bar{v}_{t_1}^{(1)} + \bar{V}_{1_{xt_3}} + \bar{V}_{2_{xt_2}} + \left(\bar{u}^{(0)}\bar{u}_x^{(0)} + \bar{v}^{(1)}\bar{u}_y^{(0)}\right)_{xy} - y\left(\bar{u}^{(0)}\bar{u}_x^{(0)} + \bar{v}^{(1)}\bar{u}_y^{(0)}\right)_{t_1}$$
$$+ y\left(\left(\bar{h}^{(0)}\bar{u}^{(0)}\right)_x + \left(\bar{v}^{(1)}\bar{h}^{(0)}\right)_y\right)_x - \left(\left(\bar{h}^{(0)}\bar{u}^{(0)}\right)_x + \left(\bar{v}^{(1)}\bar{h}^{(0)}\right)_y\right)_{yt_1}, \qquad \text{(C 63)}$$

Elimination of resonances in (C 56), thus, results in the following equation:

$$\left(\frac{\partial^2}{\partial x^2} - \frac{\partial^2}{\partial t_1^2}\right)\bar{v}_{t_1}^{(1)} + \bar{V}_{1_{xt_3}} + \bar{V}_{2_{xt_2}} + \left[\left(\bar{u}^{(0)}\bar{u}_x^{(0)} + \bar{v}^{(1)}\bar{u}_y^{(0)}\right)_{xy} - y\left(\bar{u}^{(0)}\bar{u}_x^{(0)} + \bar{v}^{(1)}\bar{u}_y^{(0)}\right)_{t_1}\right.$$
$$\left. + y\left(\left(\bar{h}^{(0)}\bar{u}^{(0)}\right)_x + \left(\bar{v}^{(1)}\bar{h}^{(0)}\right)_y\right)_x - \left(\left(\bar{h}^{(0)}\bar{u}^{(0)}\right)_x + \left(\bar{v}^{(1)}\bar{h}^{(0)}\right)_y\right)_{yt_1}\right]_{res} = 0. \qquad \text{(C 64)}$$

Here, the first, second and fourth terms do not depend on t_2, and to provide boundedness of the solution in t_2 one has to set $\bar{V}_{2_{xt_2}} = 0$. From (C 60), (C 9) we obtain

$$\bar{V}_1 = \int dt_1 \bar{v}^{(1)} = \sum_n \phi_n \int dt_1 \bar{v}_n^{(1)} = \sum_n \frac{\phi_n}{\bar{c}_n} \int d\xi\, \bar{v}_n^{(1)}(\xi) = \sum_n \frac{\phi_n}{\bar{c}_n} \bar{\mathscr{V}}_{1_n} \qquad \text{(C 65)}$$

and with the help of (C 9) we express the linear part of (C 64) as

$$\left(\frac{\partial^2}{\partial x^2} - \frac{\partial^2}{\partial t_1^2}\right)\bar{v}_{t_1}^{(1)} + \bar{V}_{1_{xt_3}} = \sum_n \frac{\phi_n}{\bar{c}_n}\left(\bar{\mathscr{V}}_{1_{n_{t_3}}} + \left(\bar{c}_n^4 - \bar{c}_n^2\right)\bar{\mathscr{V}}_{1_{n_{xxx}}}\right)_x. \qquad \text{(C 66)}$$

When analysing the resonances produced by nonlinear terms, it is important to bear in mind that only the product of a given zonal mode with itself may give rise to resonances. For example, although the long Rossby waves do mutually interact, the products of the form $\mathscr{R}_1(x+\bar{c}_1 t)\,\mathscr{R}_2(x+\bar{c}_2 t)$ are not resonant for $\bar{c}_1 \neq \bar{c}_2$ and localized $\mathscr{R}_1, \mathscr{R}_2$. Calculation of the resonant contributions corresponding to the nth meridional mode gives

$$[\ldots]_{res} = -\left(\bar{\mathscr{V}}_{1_n} \bar{\mathscr{V}}_{1_{n_x}}\right)_x \phi_n(y)\left(1-\bar{c}_n^2\right) \int \mathrm{d}y\, \frac{1}{2}\left[-\frac{P_n^-}{4}\left((P_n^-)^2 + 2\phi_n P_{n_y}^-\right) + \bar{c}_n \frac{P_n^+}{4}((P_n^+)^2 + (P_n^-)^2)\right]. \quad (\mathrm{C}\,67)$$

Therefore, the condition of absence of resonances results in the KdV equation (3.37) with the coefficients given by

$$\alpha_n = \bar{c}_n^4 - \bar{c}_n^2, \quad (\mathrm{C}\,68)$$

$$\beta_n = -\bar{c}_n\left(1-\bar{c}_n^2\right) \int \mathrm{d}y\, \frac{1}{2}\left[-\frac{P_n^-}{4}\left((P_n^-)^2 + 2\phi_n P_{n_y}^-\right) + \bar{c}_n \frac{P_n^+}{4}\left((P_n^+)^2 + (P_n^-)^2\right)\right], \quad (\mathrm{C}\,69)$$

and $P_n^{\pm}$ were defined in (C 46). Note that β_n vanishes for even n, and hence the even modes just disperse at this order. In the case of special initial conditions consisting exclusively of even meridional modes, the mKdV equation may be obtained along the same lines by changing the scaling appropriately.

Let us now define the slow evolution of the Kelvin waves. Using (C 52), (C 53) the condition (3.25) gives at this order

$$U_{0_{t_3}} + U_{1_{t_2}} + \tfrac{3}{2}\gamma U_0 U_{0_x} = 0, \quad \gamma = \int_{-\infty}^{+\infty} \mathrm{d}y\, \phi_0^3. \quad (\mathrm{C}\,70)$$

Here $U_1 = U_1(x - t_1, t_2, \ldots)$ corresponds to the first-order correction to the Kelvin-wave field. As U_0 does not depend on t_2 (cf. (C 34) and the comment after it), the same is true for U_1 and we arrive at the Riemann-wave equation (3.38).

Appendix D. Initialization procedure for $Ro = O(\delta^2)$ adjustment.

D.1. *The zeroth order*

The initial conditions for $\tilde{v}^{(0)}$ are (cf. (C 1) and (3.6) for $n = 0$)

$$\tilde{v}^{(0)}\big|_{t=0} = v_I, \quad \tilde{v}_t^{(0)}\big|_{t=0} = -\left(y u_I + h_{I_y}\right). \quad (\mathrm{D}\,1)$$

From (C 3) we then obtain

$$\tilde{v}_{n_{tt}}^{(0)} + (2n+1)\tilde{v}_n^{(0)} = 0, \quad (\mathrm{D}\,2)$$

$$\tilde{v}_n^{(0)}\big|_{t=0} = v_{I_n}, \quad (\mathrm{D}\,3)$$

$$\tilde{v}_{n_t}^{(0)}\big|_{t=0} = -\left(y u_{I_n} + h_{I_{y_n}}\right), \quad (\mathrm{D}\,4)$$

Hence, we obtain (C 5) with

$$A_{0_n}^{\pm}\big|_{t=0} = \frac{1}{2}\left(v_{I_n} \mp \mathrm{i}\frac{y u_{I_n} + h_{I_{y_n}}}{\sigma_n}\right). \quad (\mathrm{D}\,5)$$

To determine the initial conditions for $\tilde{h}^{(0)}$, $\tilde{u}^{(0)}$ we integrate (3.19), (3.21) for $n = 0$ in time:

$$\tilde{u}^{(0)} = \tilde{u}_I^{(0)} + yV_0, \;\; \tilde{h}^{(0)} = \tilde{h}_I^{(0)} - V_0. \quad (\mathrm{D}\,6)$$

Here $V_0 = \int_0^t \mathrm{d}t\ \tilde{v}^{(0)}$. By definition, the time-average of the fast fields $\tilde{u}^{(0)}$, $\tilde{h}^{(0)}$ vanishes, hence

$$\tilde{u}_I^{(0)} = -y\bar{V}_0, \quad \tilde{h}_I^{(0)} = \bar{V}_{0y}. \tag{D 7}$$

The function $\bar{V}_0$ is uniquely defined from the equation

$$\bar{V}_{0yy} - y^2\bar{V}_0 = yu_I + h_{I_y}, \tag{D 8}$$

which readily follows from (C 3) and (D 1). From (D 7), (D 8) it follows that

$$y\tilde{u}_I^{(0)} + \tilde{h}_{I_y}^{(0)} = yu_I + h_{Iy}. \tag{D 9}$$

Given $\bar{V}_0$ the initial conditions for the fast fields $\tilde{u}_I^{(0)}$ and $\tilde{h}_I^{(0)}$ follow from (D 7), (D 8) and, in turn, give the initial conditions for the slow fields:

$$\bar{u}_I^{(0)} = u_I - \tilde{u}_I^{(0)}, \quad \bar{h}_I^{(0)} = h_I - \tilde{h}_I^{(0)}. \tag{D 10}$$

It is easy to check that the initial conditions (D 10) do not contradict the geostrophic balance (C 2) because of (D 9)).

D.2. *The first order*

The slow-motion equations are

$$\bar{u}_{t_1}^{(0)} - y\bar{v}^{(1)} + \bar{h}_x^{(0)} = 0, \tag{D 11}$$

$$y\bar{u}^{(0)} + \bar{h}_y^{(0)} = 0, \tag{D 12}$$

$$\bar{h}_{t_1}^{(0)} + \bar{u}_x^{(0)} + \bar{v}_y^{(1)} = 0. \tag{D 13}$$

From (D 11)–(D 13)

$$\bar{v}_{yy}^{(1)} - y^2\bar{v}^{(1)} + \left(\bar{u}_y^{(0)} + y\bar{h}^{(0)}\right)_x = 0 \tag{D 14}$$

$$\left(\bar{u}_y^{(0)} + y\bar{h}^{(0)}\right)_{t_1} = \bar{v}^{(1)}. \tag{D 15}$$

The initial condition for $\bar{v}^{(1)}$ is obtained from (D 14), (D 15), and (D 10):

$$\bar{v}_{I_{yy}}^{(1)} - y^2\bar{v}_I^{(1)} = -\left(\bar{u}_{I_y}^{(0)} + y\bar{h}_I^{(0)}\right)_x. \tag{D 16}$$

Once $\bar{v}_I^{(1)}$ is found from (D 16), the initial conditions for $\tilde{v}^{(1)}$ to be used in (C 19) are known. The first is

$$\tilde{v}_I^{(1)} = -\bar{v}_I^{(1)}. \tag{D 17}$$

The second initial condition follows from (3.6) for $n = 1$:

$$\tilde{v}_t^{(1)}\big|_{t=0} = -\tilde{v}_{t_1}^{(0)}\big|_{t=0}. \tag{D 18}$$

To demonstrate that a Yanai wave does not contribute to the slow solution at this order we write (D 16) in the following form:

$$\bar{v}_{I_{yy}}^{(1)} - y^2\bar{v}_I^{(1)} = -\left(\left(\bar{h}_I^{(0)} - \bar{u}_I^{(0)}\right)_y - y\left(\bar{h}_I^{(0)} - \bar{u}_I^{(0)}\right)\right)_x. \tag{D 19}$$

The right-hand side of this equation may be rewritten as (cf. (A 7), (A 8))

$$\sum_{n=0}^{\infty}\left(\bar{h}_{I_n}^{(0)} - \bar{u}_{I_n}^{(0)}\right)_x(\phi_{n_y}(y) - y\phi_n(y)) = -\sum_{n=0}^{\infty}\left(\bar{h}_{I_n}^{(0)} - \bar{u}_{I_n}^{(0)}\right)_x\sqrt{2(n+1)}\phi_{n+1}(y). \tag{D 20}$$

Thus, there is no term with ϕ_0 on the right-hand side of (D 19) and $\bar{v}_0^{(1)}(x + t_1)$ vanishes, i.e. the Yanai wave is absent in (C 9). This is, in fact, a consistency check, as the Yanai wave is fast and should be contained in the solution of (C 19).

From (D 11) and (D 16) we obtain for $\bar{v}^{(1)}_{I_n}$:

$$\bar{v}^{(1)}_{I_n} = \left(\bar{u}^{(0)}_{I_{n+1}} + \bar{h}^{(0)}_{I_{n+1}}\right)_x \frac{\sqrt{2(n+1)}}{2n+1}. \tag{D 21}$$

In order to determine $F_0(x-t_1, y)$ and $G_0(x+t_1, y)$ in (C 12) we calculate $\bar{\mathscr{F}}_{0_I}, \bar{\mathscr{G}}_{0_I}$ using (C 15) and the fact that $\bar{u}^{(0)}_{I_1} + \bar{h}^{(0)}_{I_1} = 0$ following from (C 2):

$$\bar{\mathscr{F}}_{0_I}(x, y) = \bar{u}^{(0)}_I(x, y) + \bar{h}^{(0)}_I(x, y) - \left(\bar{u}^{(0)}_{I_0}(x) + \bar{h}^{(0)}_{I_0}(x)\right)\phi_0(y), \tag{D 22}$$

$$\bar{\mathscr{G}}_{0_I}(x, y) = \bar{u}^{(0)}_I(x, y) - \bar{h}^{(0)}_I(x, y). \tag{D 23}$$

From (C 12), (D 22), (D 23) we obtain

$$\bar{f}^{(0)}_I = \bar{u}^{(0)}_I(x, y) + \bar{h}^{(0)}_I(x, y) - \left(\bar{u}^{(0)}_{I_0}(x) + \bar{h}^{(0)}_{I_0}(x)\right)\phi_0(y) + F_0(x, y), \tag{D 24}$$

$$\bar{g}^{(0)}_I = \bar{u}^{(0)}_I(x, y) - \bar{h}^{(0)}_I(x, y) + G_0(x, y), \tag{D 25}$$

whence using (C 10)

$$F_0(x, y) = \left(\bar{u}^{(0)}_{I_0}(x) + \bar{h}^{(0)}_{I_0}(x)\right)\phi_0(y), \tag{D 26}$$

$$G_0 = 0. \tag{D 27}$$

D.3. *The second order*

The initial field $\bar{v}^{(2)}_I$ is found as solution of equation (3.23) for $n = 2$:

$$\bar{v}^{(2)}_{I_{yy}} - y^2 \bar{v}^{(2)}_I = -\left(\bar{u}^{(1)}_{I_y} + y\bar{h}^{(1)}_I\right)_x, \tag{D 28}$$

where $\bar{u}^{(1)}_I = -\tilde{u}^{(1)}_I$, $\bar{h}^{(1)}_I = -\tilde{h}^{(1)}_I$, and $\tilde{u}^{(1)}, \tilde{h}^{(1)}$ are known from the previous approximation.

Appendix E. Analysis of the fast–fast–slow resonances at the third order in δ

The importance of this Appendix is that it gives a proof of equatorial slow–fast splitting by a direct calculation of the nonlinear terms on the right-hand side of (C 56). Due to (C 4), (C 29), (C 5), and (C 21) we have

$$\overline{\tilde{v}^{(0)}\tilde{v}^{(0)}_y} = \sum_n \overline{\tilde{v}^{(0)2}_n}\phi_n\phi_{n_y}, \tag{E 1}$$

and

$$\overline{\tilde{v}^{(0)2}_n} = 2\left|A_{0_n}\left(x - \frac{t_1}{2\sigma_n^2}\right)\right|^2. \tag{E 2}$$

As Rossby waves move westward (cf. (C 9), (C 13), (C 14)) it thus follows that the term $(\partial^2/\partial x^2 - \partial^2/\partial t_1^2)\overline{\tilde{v}^{(0)}\tilde{v}^{(0)}_y}$ is non-resonant. Analogously, due to (C 7) we have for $\overline{\tilde{u}^{(0)}\tilde{u}^{(0)}_x}$

$$\overline{\tilde{u}^{(0)}\tilde{u}^{(0)}_x} = y^2 \sum_n \frac{\phi_n^2}{\sigma_n^4}\overline{\tilde{v}^{(0)}_{n_t}\tilde{v}^{(0)}_{n_{tx}}} = y^2 \sum_n \frac{\phi_n^2}{2\sigma_n^2}\overline{\tilde{v}^{(0)2}_{n_t}}_x \tag{E 3}$$

and

$$\overline{\tilde{v}^{(0)2}_{n_t}} = 2\sigma_n^2\left|A_{0_n}\right|^2;\ \left(\overline{\tilde{v}^{(0)2}_{n_t}}\right)_x = 2\sigma_n^2\left|A_{0_n}\left(x - \frac{t_1}{2\sigma_n^2}\right)\right|^2_x, \tag{E 4}$$

i.e. $\overline{\tilde{u}^{(0)}\tilde{u}_x^{(0)}}$ and its derivatives, entering the right-hand side of (C 56) are also non-resonant. Another average entering the right-hand side of (C 56), $\overline{\tilde{h}^{(0)}\tilde{u}^{(0)}}$, is calculated in the same way and due to (C 7) we have

$$\overline{\tilde{h}^{(0)}\tilde{u}^{(0)}} = -y\sum_n \frac{\phi_n\phi_y}{\sigma_n^4}\overline{\tilde{v}^{(0)2}_{n_t}} \tag{E 5}$$

which is again not resonant.

The average $\overline{\tilde{h}^{(1)}\tilde{v}^{(0)} + \tilde{h}^{(0)}\tilde{v}^{(1)}}$ entering $\bar{P}_h^{(3)}$ is calculated with the help of representations (C 22), (C 24), (C 4), and (C 6), (C 25). We obtain

$$\overline{\tilde{h}^{(1)}\tilde{v}^{(0)} + \tilde{h}^{(0)}\tilde{v}^{(1)}} = -\overline{\tilde{V}_{1_y}\tilde{v}^{(0)} + \tilde{V}_{0_y}\tilde{v}^{(1)}} + \overline{\tilde{v}^{(0)}\tilde{W}_{0_{yt_1}}} - y\overline{\tilde{v}^{(0)}\tilde{W}_{0_x}}. \tag{E 6}$$

We find

$$\overline{\tilde{V}_{1_y}\tilde{v}^{(0)} + \tilde{V}_{0_y}\tilde{v}^{(1)}} = -\sum_n \frac{\phi_n\phi_{n_y}}{\sigma_n^2}\overline{\left(\tilde{v}_n^{(0)}\tilde{v}_n^{(1)}\right)_t} = 0. \tag{E 7}$$

The second and the third terms in (E 6) are easy to calculate by using (C 25):

$$\overline{\tilde{v}^{(0)}\tilde{W}_{0_{yt_1}}} = -\sum_n \frac{\phi_n\phi_{n_y}}{\sigma_n^2}\overline{\tilde{v}_n^{(0)}\tilde{v}_{n_{t_1}}^{(0)}} = -\sum_n \frac{\phi_n\phi_{n_y}}{\sigma_n^2}\left|A_{0_n}\right|^2_{t_1}, \tag{E 8}$$

$$\overline{\tilde{v}^{(0)}\tilde{W}_{0_x}} = -\sum_n \frac{\phi_n^2}{\sigma_n^2}\overline{\tilde{v}_n^{(0)}\tilde{v}_{n_x}^{(0)}} = -\sum_n \frac{\phi_n^2}{\sigma_n^2}\left|A_{0_n}\right|^2_x \tag{E 9}$$

and, hence, the term $\overline{\tilde{h}^{(1)}\tilde{v}^{(0)} + \tilde{h}^{(0)}\tilde{v}^{(1)}}$ is also non-resonant.

Finally, for the average $\overline{\tilde{v}^{(1)}\tilde{u}_y^{(0)} + \tilde{v}^{(0)}\tilde{u}_y^{(1)}}$ in $\bar{P}_u^{(3)}$ from (C 23) we have

$$\overline{\tilde{v}^{(1)}\tilde{u}_y^{(0)} + \tilde{v}^{(0)}\tilde{u}_y^{(1)}} = \overline{\tilde{v}^{(1)}(y\tilde{V}_0)_y + \tilde{v}^{(0)}(y\tilde{V}_1)_y} + \overline{\tilde{v}^{(0)}\tilde{W}_{0_{xy}}} - y\overline{\tilde{v}^{(0)}\tilde{W}_{0_{t_1}}}. \tag{E 10}$$

As above, we can show that

$$\overline{\tilde{v}^{(1)}(y\tilde{V}_0)_y + \tilde{v}^{(0)}(y\tilde{V}_1)_y} = -\sum_n \frac{\phi_n(y\phi_n)_y}{\sigma_n^2}\overline{\left(\tilde{v}_n^{(0)}\tilde{v}_n^{(1)}\right)_t} = 0, \tag{E 11}$$

$$\overline{\tilde{v}^{(0)}\tilde{W}_{0_{xy}}} = -\sum_n \frac{\phi_n\phi_{n_y}}{\sigma_n^2}\left|A_{0_n}\right|^2_x, \tag{E 12}$$

and

$$\overline{\tilde{v}^{(0)}\tilde{W}_{0_{t_1}}} = -\sum_n \frac{\phi_n^2}{\sigma_n^2}\overline{\left(\tilde{v}_n^{(0)}\tilde{v}_n^{(1)}\right)_{t_1}} = -\sum_n \frac{\phi_n^2}{\sigma_n^2}\left|A_{0_n}\right|^2_{t_1} \tag{E 13}$$

This means that $\overline{\tilde{v}^{(1)}\tilde{u}_y^{(0)} + \tilde{v}^{(0)}\tilde{u}_y^{(1)}}$ is non-resonant, as well.

Thus, the stresses due to the fast motions in (C 56) do not give rise to the evolution of the slow Rossby and Kelvin waves. At the same time, they do give rise to the third-order correction of the meridional velocity.

Appendix F. A brief description of the numerical procedure and Rankine–Hugoniot conditions

The starting point is the conservation-law formulation of the equatorial RSW equations:

$$\left.\begin{aligned} h_t + (hu)_x + (hv)_y &= 0, \\ (hu)_t + (hu^2 + \tfrac{1}{2}gh^2)_x + (huv)_y &= \beta yhv, \\ (hv)_t + (huv)_x + \left(hv^2 + \tfrac{1}{2}gh^2\right)_y &= -\beta yhu. \end{aligned}\right\} \tag{F 1}$$

It is well-known that systems of conservation laws admit weak solutions with discontinuity surfaces. These solutions can be captured as solutions of a corresponding dissipative system in the limit of vanishing viscosity (the so-called *vanishing viscosity* approach, see e.g. Di Perna, 1983), or, alternatively, by specifying the cross-shock conditions, namely the Rankine–Hugoniot conditions and the entropy condition (the so-called *pseudo non-viscous* approach, see e.g. Schär & Smith 1993). A discussion of equivalence between the two approaches is also presented in that reference. Both approaches give the same solutions which consist of almost everywhere continuous field plus localized discontinuity surfaces moving with the ambient fluid velocity (*contact discontinuities*) or propagating through the fluid (*shock fronts* or *bores*). Across the bores, mass and momentum are conserved but energy dissipates (cf. e.g. Whitham 1974). A numerical scheme described below approaches shock solutions in the first way.

The system (F 1) written for the vector $U = (h, hu, hv)$ has the form

$$U_t + F(U)_x + G(U)_y = S(U). \tag{F 2}$$

Here F (G) is the flux function in the x-direction (y-direction), and S is the source term. Note that $G(U)^{\perp} = F(U^{\perp})$ where the notation $X^{\perp} = (x_1, x_3, x_2)$ is used.

Finite-volume schemes compute the evolution of a cell-centered variable $U_{i,j}$ by using the values of U in the neighbouring cells. More precisely, they calculate the *flux* between two adjacent cells (e.g. $F_{i-1/2,j}$) by using ($U_{i-1,j}$ and $U_{i,j}$)). Given the above-mentioned symmetry between F and G, in order to construct a two-dimensional scheme it is sufficient to know how to evaluate the flux for the one-dimensional Riemann problem between the states U_l and U_r for the following system:

$$\left.\begin{aligned} h_t + (hu)_x &= 0, \\ (hu)_t + (hu^2 + \tfrac{1}{2}gh^2)_x &= fhv, \\ (hv)_t + (huv)_x &= 0. \end{aligned}\right\} \tag{F 3}$$

For a homogeneous system, this procedure is called *dimensional splitting*, see LeVeque (2002). In our case, as the problem is inhomogeneous, the numerical flux function has to be discontinuous at the interface, see Bouchut (2003). The treatment of the source term is the same as in Bouchut, Le Sommer & Zeitlin (2004): we use a time-dependent apparent topography $\tilde{Z}$ such that $\tilde{Z}_x = -fv$. Thus, at each time step, we have to resolve the Riemann problem for the one-dimensional shallow-water model with topography, plus an independent advection equation for v. The topography is handled following the hydrostatic projection method of Audusse *et al.* (2003). This procedure incorporates a topographic forcing in shallow-water Riemann solvers in such a way that steadiness of stationary states is guaranteed.

We use a relaxation method of Bouchut (2003) as an approximate Riemann solver for the homogeneous shallow-water equations. Moreover, we use a relaxation solver adapted to the computation of dry beds, i.e. allowing for $h \to 0$. A general introduction to the relaxation schemes as approximate Riemann solvers is given in LeVeque & Pelanti (2001).

Finally, high-order corrections are applied: we use a second-order time-stepping scheme, the *Heun method*, see Bouchut (2003), and for spatial reconstructions the *slope limiter method*, see LeVeque (1992). We can summarize the properties of our numerical procedure as follows:

(i) second order both in space and time,
(ii) preserving stationarity of geostrophically balanced zonal flows,
(iii) conserving potential vorticity if the solution is continuous,
(iv) exactly capturing weak solutions (shocks),
(v) guaranteeing convergence when $h \to 0$.

A typical computation over 50 periods on a 200×300 grid is completed after 4000 iterations in 1 hour on a 2000MHz processor (AMD Athlon XP2400).

The idea of a dissipative vorticity change due to discontinuities in gas dynamics has been studied by Hayes (1957) and Berndt (1966). More recently this analysis was generalized by Kevlahan (1997). For the shallow-water equations, a potential vorticity jump formula was derived by Pratt (1983) in the case of straight shocks moving with a constant speed. In all of these works the along-shock momentum equation was written in a local reference frame in order to calculate the vorticity jump. Following this prescription we consider a shock (S) propagating through a material volume $V(t)$ and we introduce a local reference frame with normal and tangential unit vectors $(\boldsymbol{n}, \boldsymbol{s})$ with respect to the shock. This frame is moving at the local speed of the shock $C_n\boldsymbol{n}$. The velocity and Bernoulli function in the moving frame are

$$\bar{\boldsymbol{u}} = \begin{pmatrix} \bar{u}^{(n)} \\ \bar{u}^{(s)} \end{pmatrix}_{loc} = \begin{pmatrix} u^{(n)} - C_n \\ u^{(s)} \end{pmatrix}_{loc}, \qquad \bar{B} = gh + \bar{\boldsymbol{u}}^2/2. \tag{F 4}$$

With a notation $[A] = A_{front} - A_{rear}$ the Rankine–Hugoniot conditions are

$$\left.\begin{aligned} -C_n\,[h] + \left[hu^{(n)}\right] &= 0, \\ -C_n\left[hu^{(n)}\right] + \left[hu^{(n)2} + \tfrac{1}{2}gh^2\right] &= 0, \\ -C_n\left[hu^{(s)}\right] + \left[hu^{(n)}u^{(s)}\right] &= 0, \end{aligned}\right\} \tag{F 5}$$

where $u^{(n,s)}$ are the velocity components normal and tangential to the shock. The jump in $\bar{B}$ is obtained from the first and the second of the Rankine–Hugoniot conditions (F 5); see e.g. Lighthill (1978), where f (r) denote front (rear) state, respectively:

$$\left[\bar{B}\right] = -\frac{g}{4}\frac{[h]^3}{h_f h_r}. \tag{F 6}$$

Following the aforementioned works, we obtain the potential vorticity jump across the shock from the along-front momentum equation:

$$h\bar{u}^{(n)}\,[q] = -\partial_s\left[\bar{B}\right]. \tag{F 7}$$

For moving shocks of any shape

$$[q] = \frac{g}{4h\bar{u}^{(n)}}\partial_s\frac{[h]^3}{h_f h_r}. \tag{F 8}$$

Note that for shocks with $\partial_s\,[h]$ no change of potential vorticity is possible. We calculate the rate of change of the amount of vorticity contained in the material volume V:

$$\frac{\mathrm{d}}{\mathrm{d}t}\int_V hq\,\mathrm{d}V = -\int_{(S)} h\bar{u}\,[q]\,\mathrm{d}S = \left[\bar{B}\right]_A - \left[\bar{B}\right]_B. \tag{F 9}$$

Figure 6 shows the breaking of a Kelvin wave of depression and the subsequent PV-deposit. Choosing V to be the whole southern half-plane, the formula (F 9) suggests that negative potential vorticity will be deposited. The right hand panel confirms this result.

We should finally mention that a theory of vorticity transport due to breaking waves in rotating shallow water on the f-plane was considered recently by Bühler (2000). It was based on generalized Lagrangian-mean theory (GLM) and confirmed by numerical simulations. However, its generalization to fully nonlinear processes on the (equatorial) β-plane is difficult due to the problem of extending the standard GLM pseudomomentum definition beyond the f-plane (cf. Bühler & McIntyre 1998).

REFERENCES

Audusse, E., Bouchut, F., Bristeau, M.-O., Klein, R. & Perthame, B. 2003 A fast and stable well-balanced scheme with hydrostatic projection for shallow-water flows. *SIAM J. Sci. Comput.* (to appear).

Berndt, S. B. 1966 The vorticity jump across flow discontinuity. *J. Fluid Mech.* **26**, 433–436.

Bouchut, F. 2002 An introduction to finite volume methods for hyperbolic systems of conservation laws with source. Lectures given at CEA-EDF-INRIA Summer School on Free-Surface Shallow Flows, available at http://www.dma.ens.fr/fbouchut/.

Bouchut, F. 2003 An entropy relaxation scheme for gas dynamics and Saint Venant system that computes vacuum. Preprint DMA-ENS, Paris.

Bouchut, F., Le Sommer, J. & Zeitlin, V. 2004 Frontal geostrophic adjustment and nonlinear-wave phenomena in one-dimensional rotating shallow water. Part 2. High-resolution numerical simulations. *J. Fluid Mech.* **514**, 35–63.

Boyd, J. P. 1980*a* Equatorial solitary waves. Part 1. Rossby solitons. *J. Phys. Oceanogr.* **10**, 1–11.

Boyd, J. P. 1980*b* The nonlinear equatorial Kelvin waves. *J. Phys. Oceanogr.* **10**, 1699–1717.

Boyd, J. P. 1983 Equatorial solitary waves. Part 2. Envelope solitons. *J. Phys. Oceanogr.* **10**, 1699–1717.

Boyd, J. P. 1984 Equatorial solitary waves. Part 4. Kelvin solitons in a shear flow. *Dyn. Atmos. Oceans* **8**, 173–184.

Boyd, J. P. 1985 Equatorial solitary waves. Part 3. Westward traveling modons. *J. Phys. Oceanogr.* **15**, 46–54.

Bretherton, C. S. & Sobel, A. H. 2003 The Gill model and the weak temperature gradient approximation. *J. Atmos. Sci.* **60**, 451–460.

Bühler, O. 2000 On the vorticity transport due to dissipating or breaking waves in shallow-water flow. *J. Fluid Mech.* **407**, 235–263.

Bühler, O. & McIntyre, M. E. 1998 On non-dissipative wave-mean interactions in the atmosphere or oceans. *J. Fluid Mech.* **354**, 301–343.

Di Perna, R. 1983 Convergence of the viscosity method for isentropic gas dynamics. *Commun. Math. Phys.* **91**, 1–30.

Fedorov, A. & Melville, W. K. 2000 Kelvin fronts on the equatorial thermocline. *J. Phys. Oceanogr* **30**, 1692–1705.

Gill, A. E. 1980 Some simple solutions for heat-induced tropical circulation. *Q. J. R. Met. Soc.* **106**, 447–462.

Gill, A. E. 1982 *Atmosphere-Ocean Dynamics*. Academic.

Hayes, W. D. 1957 The vorticity jump across a gas-dynamic discontinuity. *J. Fluid Mech.* **2**, 595–600.

Kevlahan, N. K.-R. 1997 The vorticity jump across a shock in a non-uniform flow. *J. Fluid Mech.* **341**, 371–384.

LeVeque, R. J. 1992 *Numerical Methods for Conservation Laws*. Birkhäuser.

LeVeque, R. J. 2002 *Finite Volume Methods for Hyperbolic Problems*. Cambridge University Press.

LeVeque, R. J. & Pelanti, M. 2001 A class of approximate Riemann solvers and their relation to relaxation schemes. *J. Comput. Phys.* **172**, 572–591.

Lighthill, J. M. 1978 *Waves in Fluids*. Cambridge University Press.

Majda, A. 2003 *Introduction to PDEs and Waves for the Atmosphere and Ocean*, Chap. 9. American Mathematical Society.

Majda, A. & Klein, R. 2003 Systematic multiscale models for the tropics. *J. Amos. Sci.* **60**, 393–408.

Philander, S. G. 1990 *El Nino, La Nina, and the Southern Oscillation*. Academic.

Pratt, L. J. 1983 On inertial flow over topography. Part 1. Semi-geostrophic adjustment to an obstacle. *J. Fluid Mech.* **131**, 195–218.

Reznik, G. M., Zeitlin, V. & Ben Jelloul, M. 2001 Nonlinear theory of geostrophic adjustment. Part 1. Rotating shallow water. *J. Fluid Mech.* **445**, 93–120.

Ripa, P. 1982 Nonlinear wave-wave interactions in a one-layer reduced-gravity model on the equatorial beta-plane. *J. Phys. Oceanogr.* **12**, 97–111.

Ripa, P. 1983 Resonant triads of equatorial waves in a one-layer model. Part 1. Non-local triads and triads of waves with the same speed. *J. Phys. Oceanogr.* **13**, 1208–1226.

Schär, C. & Smith, R. B. 1993 Shallow water flow past an isolated topography. Part 1. Vorticity production and wake formation. *J. Atmos. Sci.* **50**, 1373–1400.

Sobel, A. H., Nilsson, J. & Polvani, L. M. 2001 The weak temperature gradient approximation and balanced tropical moisture waves. *J. Amos. Sci.* **58**, 3650–3665.

Whitham, G. B. 1974 *Linear and Nonlinear Waves*. Wiley Interscience.

Zeitlin, V., Reznik, G. M. & Ben Jelloul, M. 2003 Nonlinear theory of geostrophic adjustment. Part 2. Two-layer and continuously stratified models. *J. Fluid Mech.* **491**, 207–228.